Master thesis

Pharmacokinetic regulation of ERF, as a therapeutic approach for the ERF-related craniosynostosis in mouse

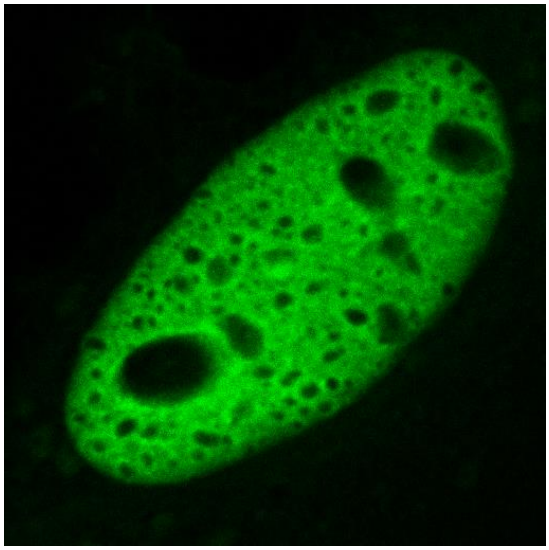

Konstantinos Makris I.D. 355

Supervisor: Prof. George Mavrothalassitis

Master program of Molecular Biology-Biomedicine

Acknowledgments

Completing my master thesis, I would like to express my gratitude to all people, who surround me in this scientific journey and for the second year of my post-graduate studies.

Hierarchically, I want to thank my professor George Mavrothalassitis, who was eager to help me in every step of this work. Having worked almost 2 and half years, I respect his scientific spirit and I believe his advice to act as the cornerstone for the rest of my scientific journey. His attitude and his scientific "ingenuity" inspire the lab members, elements which are very priceless for a mentor. I believe that he helped me to build the basis and the values that a dexterous researcher has to be equipped.

Beyond my main mentor, I want to thank the past and the current lab members for their patience and their willingness to help me both in theoretical and practical issues. First of all, I feel eternally grateful that I met Angeliki Vogiatzis (cell psychologist), who is really passionate about her job and the extensive discussions that we had about the research issues. Moreover, I am really happy about Joanna Peraki (known as Chouanita), who accomplished many things this year. Generally, she transfers her positive vibes for lab work and she is always willing to discuss, making her an invaluable collaborator. I don't want to forget the new blood of this year, Electra and Aimilia, who enriched our lab staff and I wish the best for their next steps. Their persistence reminded me that every human being has to hunt the dreams in order to come true. Also, I want to thank Angelo for his help the last 2 months, which were really painful, full of experiments. Lastly, I want to thank Elena Vorgia and Andrew Zaragkoulias as previous lab members, who embraced me when I was undergraduate student and taught me a lot of things, making the environment of the lab amusing and pleasant.

In this ending part, I want to thank of course my beloved friends and my family. Studying in Crete almost 6 years, I feel very grateful that I met good friends, who helped me and shared so many moments. Furthermore, I would like to thank my parents (Anastasio & Marina) and my brother Droso, who are the guardians of my life. I feel very lucky that my family supports and encourages my efforts and without them I will never reached at this point.

Finally, I want to thank for this year the Bodossaki Foundation for the financial support of my post-graduate studies!

Περίληψη

Κρανιοσυνοστέωση είναι η πρώιμη σύντηξη των κρανιακών ραφών, οι οποίες αποτελούν τις περιοχές ανάπτυξης του κρανίου και το επεκτείνουν μέχρι την ολοκλήρωση της ανάπτυξης. Πρόσφατα, αλληλουχίσεις ολικών εξομάτων από ασθενείς με τον συγκεκριμένο φαινότυπο, έδειξαν ότι φέρουν επικρατή απώλειας λειτουργίας μεταλλάγματα του ERF. Απλοανεπάρκεια του παράγοντα ERF οδηγεί τόσο στον άνθρωπο όσο και στο ποντικίσιο μοντέλο $ERF^{LoxP/-}$ στον συγκεκριμένο φαινότυπο. Ο συγκεκριμένος παράγοντας ανήκει στην οικογένεια ETS και έχει χαρακτηριστεί ως μεταγραφικός καταστολέας, ρυθμιστής της πλακουντογένεσης, της αιμοποίησης και της οστεογένεσης. Ανάλυση από πείραμα ChIP-seq σε MEFs, κάτω από συνθήκες πείνας, δίνουν πολλούς κοινούς στόχους οστεογένεσης του ERF με τον μάστερ ρυθμιστή της οστεογένεσης Runx2. Παράλληλα, η ιδιότητα του ERF να μεταφέρεται μεταξύ του πυρήνα και κυτταροπλάσματος, καθώς και προηγούμενες μελέτες στα μεταλλάγματα κέρδους λειτουργίας του μονοπατιού FGFR, συνηγορούν στο ότι ο συγκεκριμένος παράγοντας πιθανότατα βρίσκεται στο κυτταρόπλασμα. Δεδομένου ότι τα $ERF^{LoxP/-}$ ποντίκια εκφράζουν περίπου 30% λειτουργικού ERF, σε αυτήν την μεταπτυχιακή διατριβή επιδιώκεται η φαρμακολογική ρύθμιση του ERF στο συγκεκριμένο μοντέλο και η εύρεση καλύτερου τρόπου χορήγησης για την πιο αποτελεσματική αντιμετώπιση των προβλημάτων από τα στοιχεία του φαινοτύπου.

Abstract

Craniosynostosis is the premature ossification of the cranial sutures, which are the growth centers of the skull and expand it until the completion of the fully-maturation. Recently, whole exome seq. data from patients with this phenotype, showed that they carry heterozygous loss-of function mutants of ERF. Haploinsufficiency of ERF both in human and in the $ERF^{LoxP/-}$ mouse model lead to this particular phenotype. This factor belongs to the ETS family and is characterized as a transcriptional repressor, regulator of placenta morphogenesis, embryonic hematopoiesis, and osteogenesis. Analysis of ChIP-seq data from starvated MEFs gave a great number of common osteogenesis-related genes with the master regulator of osteogenesis Runx2. In parallel, ERF acting through nucleocytoplasmic shuttling and further insights from the gain-of function mutants of FGFR signaling, indicate that this factor is probably cytoplasmic distributed. Given the fact that $ERF^{LoxP/-}$ mice express approximately 30% of functional ERF, this master dissertation aims at regulating pharmacologically the ERF function and the finding of the best administration method for the alleviating of craniosynostosis phenotype defects.

Content

Introduction-The role of ETS transcription factors

Many cellular processes, like differentiation and development, demand the coordination and the response of many proteins, which are responsible for the regulation of the transcription. Different external (e.g. growth factors) or internal stimuli (cellular stress) lead to different activation or suppression of a mechanism, affecting downstream proteins, which can modulate the transcriptional machinery of the genes. One important transcriptional family consists of the Ets transcription factors that conquer on the genomic level, transforming the elements of transcription. There are evidence that Ets transcription factors are involved in diverse biological processes, such as cellular proliferation, differentiation, development, hematopoiesis, osteogenesis, transformation, tissue remodeling, apoptosis, regulation of the ECM and invasion.[1], [2], [3], [4]

The first founding member of the family was the v-ets gene from the *gag-myb-ets* fusion oncogene of the avian transforming E26 retrovirus which causes both erythroblastic and myeloblastic leukemias in chicken.[5] The ETS family of transcription factors enumerates 30 members and is characterized by an evolutionary-conserved DNA-binding domain, which is capable of recognizing a purine rich GGAA/T core motif in association with other transcription factors and co-factors.[1] The ETS transcription factors share the same DNA-binding ets domain, which is responsible for the binding of the core sequence and is called EBS (=Ets-Binding sequence).[1],[6] Despite the similarities of ETS factors in their ets domain, their specificities determined by the flanking nucleotides over the GGAA/T core motif.[7] The majority of Ets family members have the Ets domains in their N-terminal regions, while others contain also the so-called Pointed-domain (PNT) at their N-terminal region, which forms helix-loop-helix structurally permitting the interaction with other proteins. [1],[8] Their protein structure can possibly accommodate the activation, the autoinhibitory, the repressor, the Pointed (HLH) and the characteristic Ets domain, as shown in Figure 1.[1] Based on NMR structural data, Ets domain is composed of three helixes (α1-α3) and four-stranded β-sheets (β1-β4), which are combined in the order α1-β1-β2-α2-α3-β3-β4, forming a winged helix-turn-helix topology.[1],[9],[10] It is proven that the third α-helix has the ability of binding the DNA major groove and different flanking amino acids sequences affect the total DNA-binding affinity of the Ets proteins.[1],[7] Relevant to their function and specificity, Ets transcription factors appear some common characteristics like: (i) the uniquely tissue-specific expression profile or specific stimulatory-based response, (ii) the intracellular pathways, which constitute to the activation of some Ets factors, cause their sub-cellular compartmentalization, (iii) or change their DNA-binding affinity, (iv) or their transactivation potential, and (v) finally, different combination of Ets transcription factors and other ETS proteins can critically regulate the activity of a promoter or enhancer, in the genomic integrity.[11],[12],[13],[14],[15],[16]

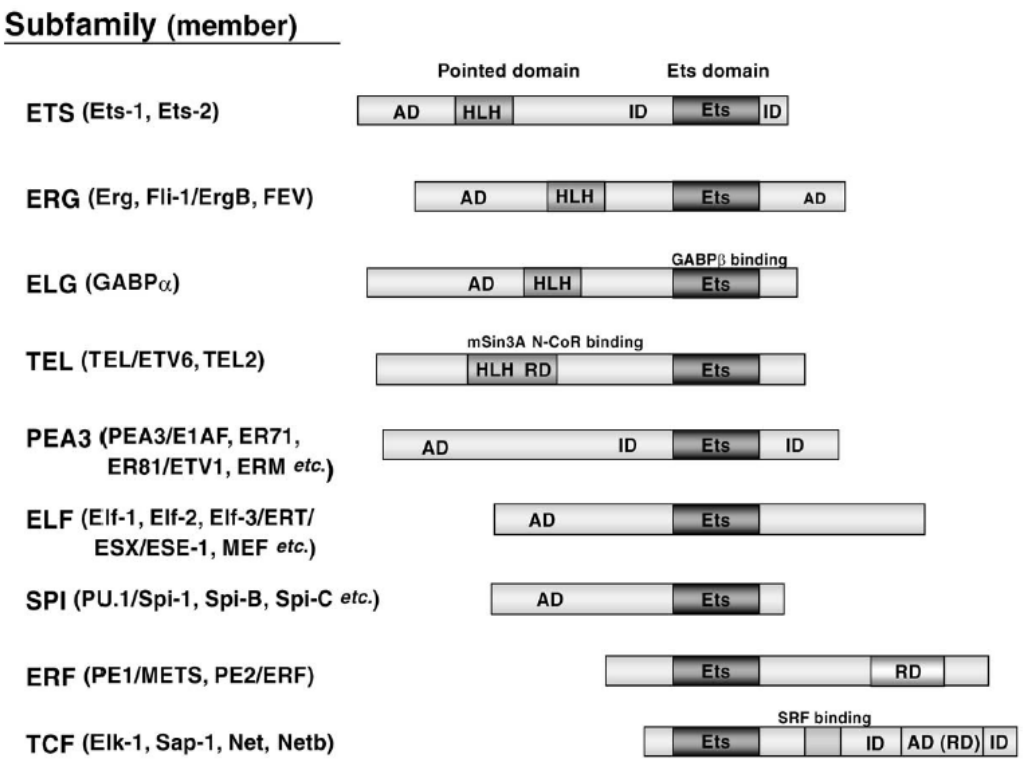

Figure 1: Schematic representation of the protein structure of Ets subrfamily. Ets, DNA-binding Ets-domain; AD, activation domain; HLH, Helix-loop-Helix domain (Pointed domain); RD, Repression domain; ID, Auto-inhibitory domain.[1]

ERF as a transcriptional repressor of Ets family and regulator of development

Within the ETS family, there are four different ETS proteins (YAN, TEL, ERF & NET) with transcriptional repressor ability.[16] One of them, ERF (ETS2 Transcription Factor) exhibits its conservative ets-DNA binding domain at the amino-terminus end, while a strong transcriptional repressor domain located at the carboxy-terminus end of the protein.[17] The 2,7kb ubiquitously expressed mRNA of ERF produces a 548 amino acid phosphoprotein, which is present in all tissues and cell lines.[17] Relevant to its inhibitory action, ERF can suppress the ETS2 promoter 30 times, while the other promoters are affinity-dependent suppressed.[17] In parallel, ERF antagonizes the other transactivators of the ets genes (like ETS1), which can reverse its repressor activity.[17], [18] Normally, ERF acts in the nucleus binding to the EBS of different ets genes.[17], [18] During the G0/G1 phase of the cellular proliferation, the phosphorylation state of this protein is established by the MAPK pathway, and more specifically by the ERK1/2 MAP kinases.[19] The recognition and the interaction between the ERF and the ERK1/2 kinases is accomplished through distinct FXF motifs.[20] The "continuous" phosphorylation of ERF in specific sites leads to the translocation of the protein from the nucleus to the cytoplasm, which is called "nucleocytoplasmic shuttling".[21] In this way, the cytoplasmic ERF is unable to exert its inhibitory action and other factors can control the ets genes.[17], [18] Upon "starvation" conditions, ERF is accumulated in the nucleus with the aim of suppressing the cellular proliferation in a Rb-dependent manner, as shown in Figure 2.[21] More specifically, nuclear ERF is capable of arresting the cell cycle at the G_0/G_1 phase.[21] When the

conditions are more favorable, ERF is phosphorylated by ERK1/2 kinases and translocates to the cytoplasm.[21] Further studies have shown that mutants of ERF in critical amino acids, which are susceptible to the phosphorylation by ERK1/2 kinases, have nuclear localization.[21] So, the phosphorylation of ERF is pivotal for the "nucleocytoplasmic shuttling".[21] The translocation of ERF from the nucleus to the cytoplasm is accomplished by the exportin XPO1/CRM1.[21] Although the exit of this protein from the nucleus is determined by the phosphorylation of specific sites, the entry is not contingent upon its phosphorylation.[21] In transcriptional level, ERF binds to the promoter of c-Myc gene repressing its transcription.[22] Beyond the nucleocytoplasmic shuttling, non-phosphorylated ERF can potentially reverse the Ras tumorigenicity and arrest cells in G1 phase.[21] Elimination of ERF during mouse embryonic development leads to the blocking of chorionic trophoblast differentiation, causing failure of the chorioallantoic fusion and embryo death (at embryonic day 10.5).[23] For successful differentiation of the trophoblast stem cells (TSCs), the presence of ERF is necessary for the inhibition of FGF2 in the syncytiotrophoblast.[24] There are evidence that elimination of ERF in the stage of epiblast (at the embryonic day E5), leads to a defect in the hemogenic endothelium, causing severe anemia at the embryonic day E14.5.[25] This lethal situation reflects its ability to modulate various processes in the mouse development. Comparing to the wild type situation, both the *ERF*$^{LoxP/-}$ mice, expressing 25-30% of normal protein, and patients with mutants in the Erf gene manifest the complex craniosynostosis phenotype.[26] So, the haploinsufficiency of ERF acts proportionally in the case of the craniosynostosis, causing both defects in the sutures of the cranial vault and craniofacial anomalies.[26] Suppressing the Semaphorin-7a, ERF can potentially regulate the process of the TGF-β induced epithelial-mesenchymal transition (the so-called EMT), restricting the behavior of cancer cells for migration.[27] The Semaphorin-7a repression by the ERF in the context of TGF-β induced EMT has given new insights about the interconnections between the TGF-β and Ras-signaling pathways.[27] Finally, new evidence that ERF regulates the prostate cancer antagonizing ERG reassure its role in the cancer progression.[28],[29]

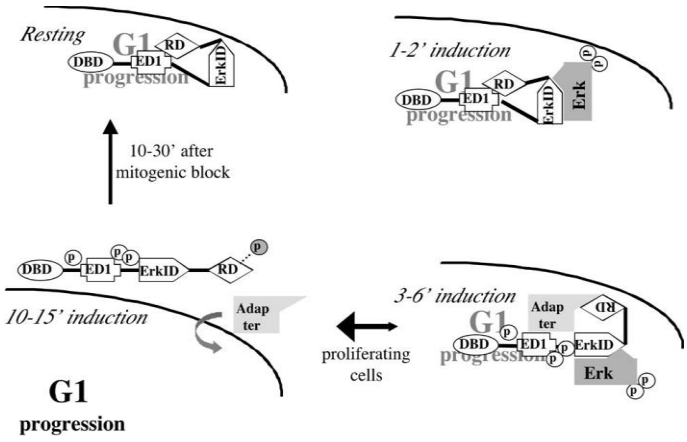

Figure 2: The ERK-dependent regulation and functionality of ERF. Upon starvation conditions, nuclear ERF suppresses the cell cycle with an Rb-dependent manner, resting the cell cycle in G1 phase. Induction with mitogenic stimuli causes the phosphorylationof ERF by the ERK kinases, leading to its cytoplasmic localization through the XPO1 exportin.[21]

KPT-330 as a potentially selective inhibitor of CRM1/XPO1

Exportin-1, also called as a chromosome region maintenance 1 (XPO1/CRM1), was first found in the *Schizosaccharomyces pombe* and is a nuclear exportin, which is responsible for the transport of various

cargoes, such as mRNAs and proteins, through the nuclear pore into the cytoplasm.[30] This ubiquitously expressed export protein belongs to the karyopherin β family.[31],[32],[33] In various malignant tumors, this protein is overexpressed, removing from the nucleus a great number of growth regulatory and tumor suppressor proteins, such as survivin, cyclin D1, APC, nucleophosmin, p53 and BRCA1/2, hence affecting the process of cell apoptosis and cell division.[34],[35],[36],[37] The use of the anti-fungal natural antibiotic leptomycin B (LMB) was an efficient way for encountering the increased levels of the XPO1/CRM1 in the diverse malignant tumors.[35],[40],[41] Binding irreversibly to the conservative cysteine residue Cys528 and preventing the binding of the RAN-GTP from the hydrophobic groove of XPO1, LMB was a potential inhibitor of nuclear export.[35],[38],[40],[41]However, the high cytotoxicity and the undesired side-effects in the phase 1 of clinical trials (such as nausea, gastrointestinal effects, and fatigue), making this inhibitor inappropriate for the in vivo use in clinical studies and for efficient therapies of cancers.[39],[42] For this reason, structural studies that have enlightened the whole structure of the export complex permitted the "in silico" design of selective inhibitors of nuclear exports (known as the SINEs).[35] The similarities of export mechanism between the human and the yeast gave the possibility for elucidating the structure of NES peptides into the cargo of CRM1/XPO1.[44],[45],[46]

The XPO1 export system requires the activation of a Ras-related nuclear G-protein (Ran), regulating both the disassembly and the binding of the candidate cargoes.[46],[47],[48],[49],[50] For the functionality of the XPO1 is necessary the establishment of RanGDP-RanGTP gradient across the nuclear envelope.[46],[47],[48],[49],[50] In the inner nuclear side, RCC1 (regulator of chromosome condensation 1) protein, as a Ran guanine nucleotide exchange factor, bound to the chromatin with histones H2A and H2B facilitates the conversion of Ran-GDP to Ran-GTP.[48],[49],[50] Comparing to the nuclear side of cells, Ran-GAP, as a GTPase-activating protein, is located to the outer cytoplasmic fibrils of the nuclear pore complex (NPC), dephosphorylating Ran-GTP into Ran-GDP.[51],[52],[53] When the ternary complexes of cargoes with the XPO1 and the elements of the nuclear pore complex are exported in the cytoplasm, then these complexes are disassembled by the dephosphorylation of Ran-GTP into Ran-GDP.[35],[51],[52],[53] The dissociation of the XPO1 leads to its recycling back to the nucleus for further rounds of exports.[35],[46],[47]

Using the structural data from yeast and human peptides with NES (Nuclear Export Signal), the newly synthesized inhibitors are more specific and selective than their ancestor, the Leptomycin B (LMB).[46],[54] For mimicking the binding groove of human CRM1/XPO1, is necessary the mutation of Thr539 of ^{Sc}XPO1 into cysteine residue for the covalent modification by the SINEs.[51] The NES peptides are 10-15 motifs, containing 4 or 5 hydrophobic residues.[55],[56],[57],[58]These amino acids are capable of forming a-helical with loops or full of loops structures in the hydrophobic groove of the XPO1.[46],[47],[55],[56],[57],[58] In the case of XPO1, the leucine-rich repeats of high molecular mass substrates are mandatory for their exports through this exportin.[46] This new class of XPO1 inhibitors are bound irreversibly to the critical Cys528 of the XPO1's hydrophobic binding groove, leading to its protein reduction.[46],[47],[54] The more reduced levels of XPO1 causing the nuclear accumulation of many tumor suppressor proteins, the more induction of the apoptosis is observed.[46],[47],[54] So, the final aim of fighting many malignancies is achieved through the reduction of the XPO1.[46],[47] During the current year, the appearance of second-generation of SINEs has given insights for their improvement in the

clinical applications.[59],[60] A characteristic example is the KPT-8602, which is unable to penetrate the blood brain barrier, having less cytotoxicity in normal hematopoietic cells and better tolerability and efficacy compared to the selinexor (KPT-330).[59],[60] So, the SINEs are evolving as new selective drugs for the fight of many aggressive cancers.[59],[60]

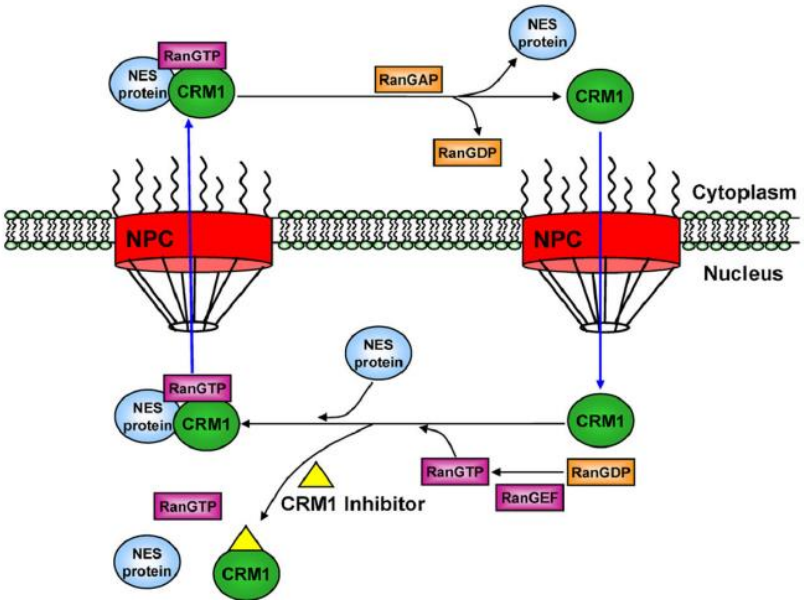

Figure 3: The Ran system of the nuclear export of cargo proteins recognizes the NES peptides and transfer them into the cytoplasm by using the CRM1/XPO1. For the transport of protein through the Nuclear Pore Complex (NPC), is necessary the phosphorylation of RanGDP by the RanGEF, a Ran nucleotide exchange factor, while the RanGAP (a Ran GTPase activating factor) dephosphorylates the NES protein releasing it into the cytoplasm. [47]

U0126 as a highly selective inhibitor of the MAPK pathway

Extensive work in the ERK-MAPK pathway indicates that ERK1/2 (extracellular signal-related kinases) is involved in many cellular processes, such as meiosis, mitosis, differentiation, and apoptosis.[61] Among the different signaling cascades (BMP/Smad, Hedgehog, and Wnt/β-catenin), ERK kinases are intracellular molecules that are phosphorylated at a threonine residue and an adjacent tyrosine residue by the MEK1/2 kinases.[61] Generally, an external stimuli (cytokine or growth factor) activates an upstream MAPK kinase kinase (MAPKKK-Raf), which is responsible for the phosphorylation and activation of a MAPK kinase (MAPKK-MEK1/2), and in turn, phosphorylates the extracellular-signal regulated MAPK kinase (ERK1/2).[62] Structural data have shown that the phosphorylation of the threonine and tyrosine residues in the T-loop of ERK1/2 is a prerequisite for their activation by the MEK1/2.[63] Moreover, the combination of the proper residues in the T-loop and the native ERK1/2 tertiary structure permits their recognition and their subsequent phosphorylation.[63] Until now, MEK1/2 are the only known upstream kinases of ERK1/2 substrates.[63],[64] Also, MEK1/2 kinases appears to be in at least two activity states (high and low) which are discernible by their phosphorylation status.[63] Among the different designed MEK inhibitors, U0126 and PD325901 are the most specific and well-studied (Figure 4).[63] Both of them are non-ATP competitive inhibitors and thermodynamic analysis have shown that they contribute to the stabilization of the MEK protein conformation.[63] Compared to the synergistic stabilization of MEK1 by the PD325901, U0126 has direct stabilization effect.[63] For this

reason, is selected for the majority of studies both in mesenchymal stem cells and craniofacial diseases.[63]

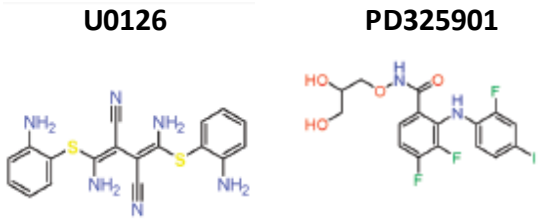

Figure 4: Two-dimensional structures of U0126 and PD325901.[63]

Albeit, MAPK pathway plays pivotal role in neuro-cardio-facio-cutaneous (NCFC) syndromes and various cancer types, the development of MEK inhibitors is potentially a way of controlling the effects from these phenotypes.[65],[66] The family of NCFC syndromes includes Neurofibromatosis type 1 (NF1), Noonan, Costello, Cardio-face-cutaneous (CFC) and LEOPARD syndrome which are aberrant Ras-related developmental disorders.[65],[66] The first evidence that U0126 is potentially an inhibitor of facial abnormalities was shown in the case of Noonan syndrome.[67] Furthermore, another characteristic example of rescued phenotype by the MEK inhibitor is Apert syndrome, which is categorized in craniosynostosis models.[68] In embryogenesis, sustained activation of ERK1/2 kinases in the neural crest cells leads to reduced osteogenic differentiation.[67],[69] So, administration of U0126 causes temporal activation of ERK1/2, permitting the normal development of face and skull.[67],[69] Compared to the various developmental stages, inhibition of ERK through U0126 suppresses the osteogenesis both in adult human MSCs and mouse MC3T3-E1 preosteoblastics cells.[70],[71] However, in the case of rat bone marrow mesenchymal stem cells (BM-MSCs), U0126 promotes the osteogenesis in a BMP-Smad dependent manner.[61] The inactivation of ERK signaling by the U0126 inhibitor promotes the phosphorylation of Smad1/5/8, leading to osteogenic differentiation.[61] Based on various evidence, U0126 is potentially a drug that regulates osteogenesis.[61],[70],[71] Furthermore, U0126 does not affect adipogenesis, while enhances the osteoclastogenesis.[72],[73] Generally, MAPK inhibitors promote the differentiation of Raw264.7 cells into osteoclasts-like cells, while p38 inhibitors suppress it.[73] Consequently, use of U0126 is also positive for the differentiation program of pre-osteoclasts, giving permission for increased activation of p38 and subsequently contributing to the increased number of $TRAP6^{+}$ positive cells.[73] Based on the aforementioned results, U0126 reduces the levels of phosphorylated ERK1/2 kinases, affecting the MSCs, the differentiation program of both osteoblasts and osteoclasts, making this drug a potentially pharmacological regulator of ERK signaling in bone homeostasis.

Anatomy of the cranial vault and bone homeostasis

In vertebrates, calvarium is a complex structure, which is composed by the neurocranium and the viscerocranium.[74] Neurocranium surrounds and protects the brain, while the viscerocranium has supportive role in nutrition and respiration.[74] Neurocranium gives birth in facial structures, which come from endochondral ossification, while the viscerocranium, through intramembranous

ossifcation, produces the cranial vault.[74] In the borders of the membranous bones, there are discrete regions, the sutures which are the growth centers of the skull.[74],[75] Through intramembranous ossification, the mesenchymal stem cells and osteoprogenitors differentiate and expand the skull, giving enough space for the growing brain.[74],[75] In the human and mouse cranial vault, there are 5 different anatomical sutures: (i) the metopic or anterior-frontal suture, (ii) the sagittal suture, (iii) the coronal suture, (iv) the labdoid suture, and (v) the supraoccipital suture (*Figure 5*).[74],[75] Both human and mice share the same anatomical cranial structure.

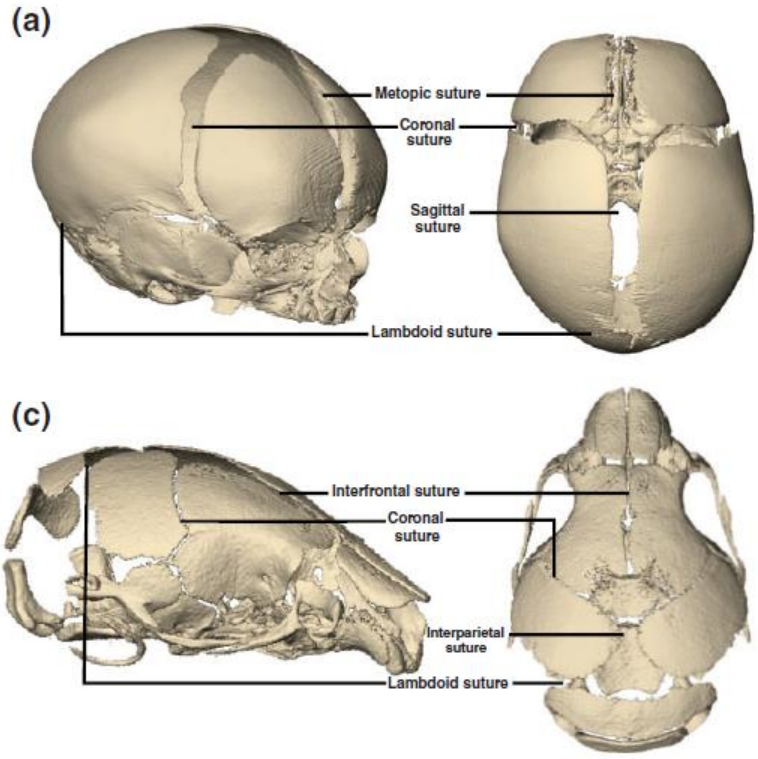

Figure 5: Cranial anatomy of (a) human and (c) mouse.[74],[75]

Developmentally, the end of gastrulation is accompanied with the formation of the three embryonic layers (the mesoderm, endoderm, and ectoderm) and signals the inaugural migration of a forth layer emerged by the folding of the neural crest.[76],[77] During the migration of the neural stem cells, has been observed the closure of the neural tube and the folding of the neural ruffles.[76],[77] In mice, the migration of neural crest cells starts at embryonic day 8 (E8) and lasts about 2 days.[76] In human, this process starts at embryonic day 19 (E19) and finishes at embryonic day 38 (E38).[76] The migration of neural crest cells occurs 5 days before the appearance of the mandible and is completed 7-8 days after the formation of the first cranial bone plate.[76],[78] After the completion of the neural crest cell migration, mouse head is composed of both paraxial mesoderm and neural-crest derived regions.[76],[77],[78] Relevant to the cranial bone homeostasis, osteogenesis and osteoclastogenesis are the key processes for the formation of cranial bones.[79] Furthermore, osteoblasts can be differentiated into osteoblasts either using endochondral or intramembranous ossification.[79] Intramembranous ossification is the direct differentiation of mesenchymal progenitors into osteoblasts, while endochondral ossification can lead to the differentiation of hypertrophic chondrocytes into osteoblasts.[79] In the frame of the

endochondral ossification, the condensation of mesenchymal progenitors leads to the formation of chondrocytes (cartilage cells) and perichondrial cells.[76] Perichondrial osteocytes can differentiate directly into osteoblasts, while chondrocytes exit from the cell cycle and grow in size.[79] When they are in a hypertrophic state, they switch into osteoblasts through the activation of Indian Hedgehog signaling (as shown in Figure 6).[79] Finally, mesenchymal progenitors can differentiate into osteogenic, chondrogenic, and adipogenic fate, while hematopoietic stem cells are the precursors of the osteoclasts-derived cells.[79]

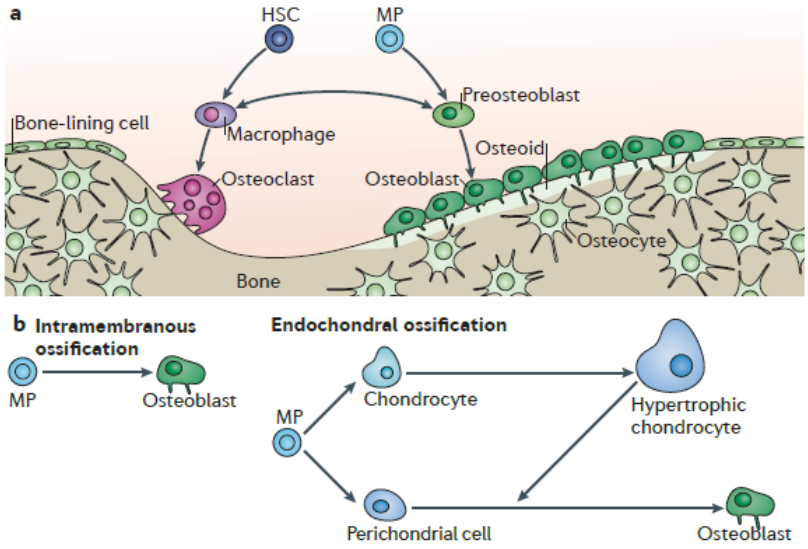

Figure 6: The bone homeostasis and the processes of intramembranous and endochondral ossification.[79]

The pathogenesis of craniosynostosis disease

Craniosynostosis is the most common craniofacial disease in human, affecting approximately 1 to 2.100 newborns.[80],[81] This disease is characterized by the premature ossification of the cranial sutures, which are the growth centers of the skull.[80],[81] Premature ossification of these regions causes abnormal growth of the skull and the compensatory changes reform it, as well as the growing brain.[80],[81] Consequently, patients with craniosynostosis exhibit mental problems due to increased intracranial pressure into different brain regions and sometimes they present facial phenotype.[80],[81] Moreover, the craniosynostosis disease can be syndromic and non-syndromic.[80],[81] In the majority of craniosynostosis cases, both human and mice have gain of function mutants in the FGFR signaling.[80],[81] Given the fact that FGF-R receptors are the upstream factors, their constitutive activation leads to the whole activation of cascade from the embryogenesis.[80],[81] So, the constant activation of FGFR signaling is a major cause of craniosynostosis phenotype, starting from the embryogenesis state.[80],[81] More specifically, gain of function mutants in FGFR-1,-2, and -3 has been correlated with syndromes, such as Pfieffer, Apert, and Muenke, respectively.[80],[81] However, each craniosynostosis case is specific and mutations even in downstream factors, such as Twist, TCF12, and ERF, are potentially responsible for the pathophysiology of disease.[26],[80],[81],[82],[83]

In the context of ERF complex craniosynostosis, haploinsufficiency of ERF leads to this phenotype.[26] Whole exome sequencing data from patients, carrying loss-of function mutants, and ERF$^{LoxP/-}$ mice, which express approximately 30% of normal WT protein, indicate the craniosynostosis phenotype.[26] Previous studies in the FGFR craniosynostosis mouse models have shown that enhanced activation of ERK1/2 kinases is a cause for constitutive phosphorylation of their substrates.[67],[68],[84] Considering that ERF is a substrate of ERK1/2 kinases and phosphorylation is the key modification signal for its export, it is speculated that probably ERF is phosphorylated.[19],[26] Because of its nucleocytoplasmic shuttling, this 30% of WT ERF is mainly accumulated in the cytoplasm.[19],[26] The absence of ERF in the nucleus, which may be a regulator of osteogenesis, changes the ossification program of sutures.[26] Beyond the role of ERF in the cranial vault physiology, patients and mice exhibit facial phenotypical traits, such as hypoplasia of their midface, hypertelorism (which is the broadened distance between the eyes), prominent forehead and orbits, and shortened and/or vertical rearrangement of their nose.[26] Also, due to increased intracranial pressure they perform Chiari malformation, language delay, and lack of appetite (as shown in Figure 7).[26] Elucidating the role of ERF in the ossification program and its involvement in the suture closure will give therapeutic approaches for the fighting of this disease. Finally, this current work has the aim of finding therapeutic strategies for the alleviation of ERF-related craniosynostosis phenotype effects in mice.

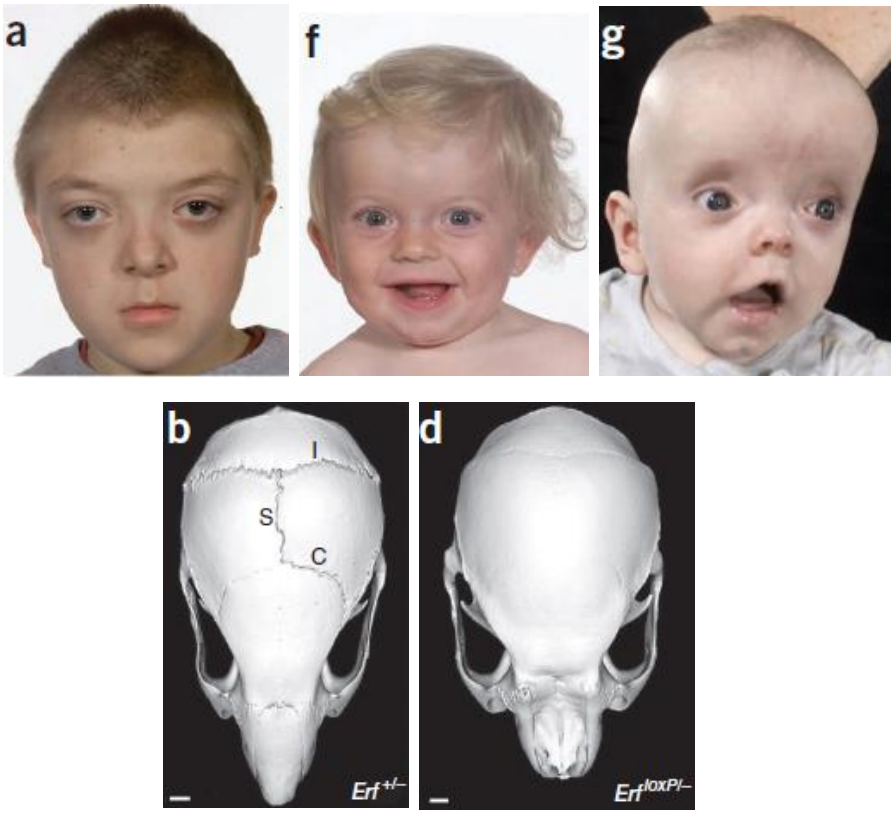

Figure 7: Craniosynostosis patients and ERF$^{LoxP/-}$ mouse model. In figure a, f, and g patients present both closure of sutures and facial phenotype, such as hypertelorism (a), Prominent forehead and orbits (f, g) and generic hypoplasia of their midface (a, f, and g). Also, ERF$^{LoxP/-}$ compared to ERF$^{+/-}$ mice exhibit multisuture synostosisand shortened nose (b and d).[26]

Aims of studies:

This master thesis targets of answering if pharmacological regulation of 30% functional ERF in the $ERF^{LoxP/-}$ mice can potentially alleviates from the craniosynostosis phenotype. This pharmacological study aims of elucidating the following subjects:

- Pharmacological inhibition of ERF translocation, through subcutaneous administration of KPT-330 inhibitor in the cranial vault, can improve the craniosynostosis phenotype.
- Pharmacological regulation of ERF phosphorylation status, through subcutaneous administrations of U0126 in the cranial vault, can improve the craniosynostosis phenotype.
- Subcutaneous administration of inhibitors in the cranial vault can act as a local administration, while intraperitoneal administration is a systemic administration method for the case of these inhibitors.
- These pharmacological therapies can affect the overall growth of mice.
- Upon MEK inhibitor, there are reduced levels of p-ERK1/2 kinases in the different administration methods.

Materials and Methods

Administration of drugs in mice. Mice were born and were bred both in Animal Facility of IMBB and Faculty of Medicine. The breeding was between females $ERF^{+/-}$ and males $ERF^{LoxP/LoxP}$ mice in order to give birth $ERF^{LoxP/-}$ and $ERF^{LoxP/+}$ mice in ratio (1:1). At postnatal day 5^{th}, newborn pups were injected subcutaneously in their cranial vault either with 0.5mg/kg of U0126 diluted in (1:1) DMSO/PBS 1X or 0.5mg/kg of KPT-330 diluted in 100% DMSO. The subcutaneous injections with these drugs were done every other day until the completion of their adulthood and the mice were sacrificed approximately at the postnatal day 65^{th}. The injections were accomplished using a Hamilton syringe and doing injection with ranging volumes between 2.5 and 4 μl. The control groups were injected with (1:1) DMSO: PBS 1X every other day with the same way. Mice were killed via cervical dislocation.

DNA extraction from mouse tails. Before the genotyping, mice were marked and a small piece from their tails was used for the DNA extraction. Tailing was performed between the postnatal day 10^{th} and postnatal day 15^{th}. The procedure of DNA extraction starts using 150-200 μl of lysis buffer (25mM NaOH, 0.2mM EDTA, pH=12) for 10-15 min incubation time, at 95 °C. After the boiling of the tails, it follows the equilibration of pH, adding (equal volume) 150-200μl of neutralization buffer (40mM Tris-HCl, pH=3.5). Afterwards, a full spin centrifugation at 13000rpm for 1 min causes the precipitation of cell debris and protein complexes and samples are ready for genotyping.

Genotyping of mice using PCR (Polymerase Chain Reaction). For the identification of the $ERF^{LoxP/-}$ and $ERF^{LoxP/+}$ mice, there are two different existed PCR protocols. The first protocol is referred to the detection of loxP sites and the wt allele and it produces a 200bp band from the allele that carries the loxP sites, while the wt allele gives a 160bp band. The second protocol is referred to the detection of the deleted ERF gene. Generally, the ablation of the loxp sites gives a 200bp band, while the wt allele does not give a product.

PCR for loxP ERF (1^{st} protocol)	*PCR for deletion (2^{nd} protocol)*	*PCR programme settings*
1μl DNA (30 ng/μl)	1μl DNA (30 ng/μl)	1. 93 °C, 2 min
2.5μl 10 x buffer E Invitrogen	2.5μl 10 x buffer F Invitrogen	2. 93 °C, 30 sec
0.5μl dNTPs (40mM)	0.5μl dNTPs (40mM)	3. 56 °C 20 sec
0.5μl m11671F (25μM)	0.5μl 4021 F (25μM)	4. 72 °C, 30 sec
0.5μl 11771R (25μM)	0.5μl 11771R (25μM)	5. GoTo 2, 34 cycles
0.5 μl DMSO	0.5μl Taq	6. 72 °C, 3 min
0.5μl Taq polymerase Minotech	19.5μl dH_2O	7. 4 °C, for ever
19μl dH_2O	V_F= 25μl	
V_F= 25μl		

m11671F: 5'-ACG CCA CAG CCC AAC TCT CC - 3'

11771R primer : 5' –CAGCAAAAGCTCAGGGAGTG- 3'

4021F primer : 5' –GCACTGCTAGCTCTGAATGG- 3'

Alcian Blue and Alizarin Red S staining. After the completion of the experiments, skulls were stained with the protocol for the staining of cartilage using Alcian Blue and the staining of bones using Alizarin Red S, respectively. Afterwards, the removal of brains was followed and the skulls were placed in 50 mL tubes containing 90% ethanol for one day under gentle agitation. Afterwards, specimens were fixed in 96% ethanol for at least 10 days and then were transferred in acetone for about 3 days. The next was the staining with Alizarin Red/ Alcian Blue staining solution for 10 to 14 days. The staining procedure (as well as the following steps) took place in dark and the solution was changed on a regular basis. Stained samples were hydrated by immersion using sequentially decreasing concentrations of ethanol (90%, 70%, 40% and 15%) for more than 1 hour per incubation and rinsed with dH2O until they sunk. Upon hydration, specimens were cleared from the remaining tissues using 1% potassium hydroxide (KOH) and replacing glycerol - 1% KOH solutions of ascending concentration (20%, 50% and 80%). It should be highlighted that the reported incubation times were adjusted when it was necessary. Finally, skeletal preparations were stored in 100% glycerol in dark.

Morphometric analysis of skulls. Stained skulls were observed under steoreomicroscope (Leica MZ12) and digital images were captured using a Canon Powershot G6 camera. Linear distance measurements were calculated from cranial landmarks (as defined by Kawakami and Yamamura 2008) using ImageJ software. A ruler was photographed together with each skull as a size standard in order to re-adjust the size of the structures. Among the groups, the measurements were compared in order to observe the differences between the treated versus the untreated mice.

Extraction of proteins from mouse cranial vaults. Extracted cranial vaults were embedded in liquid nitrogen, and using a pestle, they were homogenized. After the completion of the homogenization, they transferred in 15 ml tubes and waiting for the removal of liquid nitrogen, it follows the addition of RIPA buffer (50mM Tris-HCl, pH=8, 150mM NaCl, 1% v/v NP-40, 0.5% w/v DOC, 0.1% w/v SDS, and a cocktail of protease and phosphatase inhibitors) for the extraction of proteins. In order to help RIPA buffer for the extraction of proteins, use of vortex is necessary for some seconds. The next step was the centrifugation of samples at full spin in 13000rpm, for 20 min, at 4 °C. Finally, the transfer of supernatants was accomplished into new 1ml eppedorfs and the storage of them was done at -80 °C.

Estimation of protein concentration. Concentration of protein extracts were estimated using Bradford assay. The Bradford assay contains 800μl d. H_20, 200μl of 5X Protein Assay Dye Reagent (Bio-Rad), and a range of 5-10μl of protein sample. For the elimination of the background in the photospectrometer, it is necessary the use of a blank sample, which contains 5-10μl of RIPA buffer instead of sample. Afterwards, the photospectrometer is ready to measure the absorbance of dye, at 595nm. Based on the standard curve of 1% BSA and the measured absorbance, is feasible the estimation of protein concentration.

Western Blot. The protein samples were prepared in the desired quantity mixed with the 1X loading buffer in the final concentration and were boiled for 10 min, at 95 °C. Afterwards, the boiled proteins are denatured and centrifugation (in 13000rpm, for 1min, RT) of samples is necessary for their accumulation in the bottom of the eppedorfs. The next step was the loading of samples in a 4% stacking/10% separating

SDS-PAGE gel and the electrophoresis of gel. As protein ladder for the estimation of molecular weight of protein samples, was loaded the dye "*SeeBlue® Plus2 Pre-Stained Standard* by Life Technologies or *BenchMark™ Pre-Stained Protein Ladder by Invitrogen".* The electrophoresis of gel was done at approximately 100V and 40 mA. After the running of samples in the SDS-PAGE gel, the isolation of separating gel and subsequently the transfer of proteins in a nitrocellulose membrane *(Protran® BA-85 by GE Healthcare*) was accomplished, through a semi-dry protocol. For the semi-dry conditions, the embedment of 4 Whatman paper sheets and 1 nitrocelullose membrane in Transfer buffer is mandatory. Making a "transfer sandwich", starting from the cationic side of a SEMI-PHOR^{TM} transfer apparatus and putting with the following row 2 Whatman paper sheets, the nitrocellulose membrane, the separating gel, and the 2 other Whatman paper sheets. The duration of the transfer was 120 minutes and the applied current was 0.8 mA/cm^2 of the nitrocellulose membrane. After the completion of transfer, the nitrocellulose membrane was left at RT for 20min for the better fixation of the protein and incubation with the blocking buffer for 1h can eliminate the possible non-specific interactions of proteins with the upcoming incubating antibodies. The incubation with the blocking buffer was done under gentle agitation on an orbital shaker. For the recognition of the desired proteins, membrane was incubated in a solution with the primary antibodies diluted in TBS 1X – 0.05% Tween20 (TBS-T), overnight. Next day, the three washes with TBS-T for 15 minutes and incubation with the secondary antibody for 1 hour at RT was performed. Usually, secondary antibody is conjugated with the HRP. Finally, 3 more washes with TBS-T for 15 min were performed and detection of HRP activity was done using the ECL substrate for 2-5 min. For the detection of the chemiluminesence, images were obtained by the Gel Doc XR+ System of BioRad and they were processed with Image Lab™ software.

Mammalian Cell culture-cell culture of HeLa cells. HeLa cells is an immortal cell line coming from the human cervical carcinoma. Generally, these cells were grown in T75 flask in DMEM low glucose medium (1 gr glucose/ liter, Gibco by Life Technologies) supplemented with 50 units/mL penicillin/ streptomycin (Gibco by Life Technologies) as well as 10% Fetal Bovine Serum (Gibco by Life Technologies). The maintenance of these cells was held in a humidified incubator at 37 °C, 5% CO_2.

Passage of cells. In the case of HeLa cells, they are adherent and they sit down in the bottom of the flask, forming a monolayer. When the confluency of the flask was approximately 100%, the cells were ready for the next passage or transfer into another flask. Before the use of reagents, trypsin and medium were heated in order to be warm and ready for use. The use of aspirator aims of removing the existed medium and washing of cells with PBS 1X is compulsory for the removal of the medium between the cells since medium inhibits trypsin activity. When the cells are clean, then 5 min incubation with the trypsin-EDTA 0.25% Gibco (by Life Technologies) causes the detachment of cells from the plastic bottom of the flask. In the majority of case, the addition of 5 ml medium for the deactivation of trypsin was performed and the selection of cells was done in a 15 ml falcon tube. In order to remove the medium with trypsin, the centrifugation at 300-400g for 3 min, at RT is adequate to accumulate the cells in the form of pellet. Using again aspirator for the removal of supernatant, it follows the resuspension of the cell pellet in 10ml of new medium, the counting of cells via a hemocytometer, and the dilution of cells in order to seed the desired number of cells into the next flask.

Transfection with calcium phosphate ($CaCl_2$). One day before the transfection protocol, the cells were plated at 1-1.5*10^5 cells/well (for a 6 well-plate) and 1*10^4 cells/well (for a 24 well-plate). Moreover, coverslips were sterilized under the fire and they plated one per well. Next day, the cells are ready for the transfection. Before the addition of the sediment, the change and 1-4h incubation with new medium and 10mM HEPES is mandatory for the equilibration of pH cells. HEPES is a substance that deters the pH changes in the medium. After the 1-4h incubation, the preparation of the sediment was performed in the lab. For the in vitro studies, the sediment contained the plasmid vector, expressing the GFP-ERF fusion protein. As carrier DNA, was also used herring sperm DNA, which enhanced the total quantity of DNA for the formation of the sediment. The whole concept of the calcium phosphate protocol depends on the formation of a DNA-calcium sediment, which helps the uptake of DNA through the process of endocytosis. The procedure is the following and is referred to a well (of a 6 well-plate). Firstly, 1μg of plasmid GFP-ERF DNA and 3μg of carrier DNA were diluted in 75μl n.H2O and equal volume (75μl) of 0.5 M $CaCl_2$ solution was added to the mix of DNA. After gently mixing, 150μl of cold Solution H was added in the center of the well and adding the solution of DNA/$CaCl_2$ (150μl) dropwise in order to enhance the exchange of phosphate and potassium anions. The resulting mixture was pipetted up and down and incubated for 20 min. at room temperature so as the calcium phosphate-DNA precipitate was formed. Finally, the addition of the 300μl in 3 ml of medium was the final step for the completion of the protocol.

Cell fixation, nuclear staining, and mounting. Fixation of HeLa cells was accomplished either using RT incubation with 4% PFA (Paraformaldehyde) or incubation with (1:1) Methanol-Acetone at -20 °C, for 10 min. After the incubation with the fixatives, it follows the washing of cells with PBS 1X and their staining with a nuclear dye, such as DAPI and TOPRO3. DAPI (4', 6-diamidino-2-phenylindole) is a fluorescent dye that is intercalated into the AT rich regions of the DNA, while TO-PRO-3 is a nuclear dye that intercalates into the double strand DNA. In the end, cells are mounted in the slides using Mowiol solution and are ready for observation in SP2 Confocal microscope.

Titration of drug from mouse blood. Firstly, the injections in mice were performed and their blood collection was accomplished after 2 and 6 hours. At 2h, the collected blood, which was approximately 60 μl was mixed with 60 μl of PBS 1X with heparin in final concentration 5 units/ml. At 6h, the collected blood, which was approximately 60 μl was mixed with 60 μl of PBS 1X with heparin in final concentration 5 units/ml. The blood samples were kept on ice and they were centrifuged at 5000 rpm, for 15 min, at 4 °C. After the centrifugation, the supernatants were transferred into new tubes and were kept at 4 °C. The next day, these quantities were diluted at 1/10 ratio and 3 times sequentially with medium at ½ ratio and transfected HeLa cells in coverslips (in a 24 well-plate) were incubated in these quantities. After the passage of 2 hours, cells were fixed and stained for observation.

Statistical analysis. All data were expressed as means ± standard deviation. The statistical significance of all data from mice were determined in Microsoft Office Excel (2008) using one-way ANOVA and t-tests were corrected by post-hoc Bonferroni test. Differences were considered as statistical significant at *$*P<0.05$*, *$**P<0.01$*, and *$***P<0.001$*.

Reagents and solutions

Skeletal (Alcian Blue and Alizarin Red S) staining

1 volume of 0.1% w/v Alcian Blue diluted in 70% ethanol
1 volume of 0.1% w/v Alizarin Red S diluted in 50% ethanol
1 volume of glacial acetic acid
17 volumes of 96% ethanol

Buffers for DNA assays

For DNA extraction from mouse tails

Buffer 1: 25mM NaOH, 0.2mM EDTA, pH=12

Buffer 2: 40mM Tris-HCl, pH=3.5

For DNA electrophoresis

TBE 5X:	445mM Tris-HCl, pH=8 445mM Boric acid 10mM EDTA
DNA loading buffer 10X:	80% v/v glycerol 100mM EDTA 0.1% w/v Orange G dye

For protein extraction

RIPA buffer:	50mM Tris-HCl, pH = 8 150mM NaCl 1 % v/v NP-40 0.5 % w/v DOC 0.1 % w/v SDS 200mM Tris-HCl, pH=6.8 8% w/v SDS
SDS loading buffer 4X:	40% v/v glycerol 4% v/v mercaptoethanol 0.04% w/v bromophenol blue
4% acrylamide gel: (Stacking gel)	3.63mL dH2O 0.67mL 30% acrylamide/ 0.8% bis-acrylamide 0.625mL 1 M Tris-HCl, pH = 6.8 50µl 10% w/v SDS 5µl TEMED 50µl 10% w/v APS

10% acrylamide gel:	4.02ml d.H_20
(Separating gel)	3.28ml 30% acrylamide/ 0.8% bis-acrylamide
	2.5ml 1.5M Tris-HCl, pH=8
	100µl 10% w/v SDS
	10µl TEMED
	100µl 10% w/v APS
Running buffer 10X:	250mM Tris
	2M glycine pH=8.3
	1% w/v SDS
Transfer buffer:	20mM Tris
	160mM glycine
	0.08% w/v SDS
	20% v/v methanol
TBS 10X:	0.5M Tris-HCl, pH=8
	1.38M NaCl
	27mM KCl
TBS-T:	50mM Tris-HCl pH=8
	13.8mM NaCl
	2.7mM KCl
	0.05% v/v Tween 20
Blocking solution:	5% w/v non-fat milk diluted in TBS-T

Buffers/Media for mammalian cells

Freezing medium 2X:	20% v/v DMSO
	20% v/v FBS
	60% culture medium
HBS 10X:	1.37M NaCl
	50mM KCl
	7mM Na_2HPO_4
	6mM Dextrose
	274mM NaCl
	5mM KCl
Solution H:	1.4mM Na_2HPO_4
	1.2mM Dextrose
	200mM HEPES

Primary Antibodies

- S17S rabbit polyclonal antibody. This antibody was generated against peptides derived from the carboxy-17 amino acids of the ERF and was subsequently purified by affinity chromatography. The antibody was diluted in TBS-T and was used in (1:1000) dilution

- Rabbit monoclonal anti - p44/42 MAPK (Erk1/2) antibody (Cell Signaling, product number 4695). The antibody was diluted in TBS-T and was used in (1:2000) dilution.

- Rabbit monoclonal anti - phospho-p44/42 MAPK (Erk1/2) (Thr202/Tyr204) antibody (Cell Signaling, product number 9101). The antibody was diluted in 5% BSA - TBS-T and was used in 1:1000 dilution.

- Mouse anti – β tubulin antibody (Kindly provided by Theodoropoulos' Lab). The antibody was diluted in TBS-T and was used in (1:2000) dilution.

Secondary Antibodies

- Goat anti–rabbit horse radish peroxidase conjugated antibody diluted in TBS-T and was used in (1:5000) dilution.

- Goat anti–mouse horse radish peroxidase conjugated antibody diluted in TBS-T and was used in (1:5000) dilution.

Results

Subcutaneous administration of U0126 alleviates the suture closure in ERF$^{LoxP/-}$ mice

As previously mentioned, MEK inhibitor U0126 has been used for the rescue of craniosynostosis in Apert syndrome and in craniofacial disease of Noonan syndrome.[67],[68] MEK inhibitor reduces the levels of p-ERK1/2 kinases and subsequently reduces the phosphorylation of ERF, which is the key signal for its export into the cytoplasm (*Figure 1a*).[19],[26] Administration of MEK inhibitor causes the reduced phosphorylation of ERF with the aim of accumulating in the nucleus and facilitating its role in the developmental program of sutures. In the case of ERF-complex craniosynostosis, starting at postnatal day 5th and continuing subcutaneous injections of 0.5mg/kg U0126 every other day until the completion of the mice adulthood, they were sacrificed at postnatal day 65th (*Figure 1b*). After the staining with Alcian & Alizarin Red S, they were assessed for their suture patency in their cranial vault. Compared to the untreated ERF$^{LoxP/-}$ mice, treated group has more opened coronal and sagittal sutures. Moreover, quantification of their suture width has shown that there is rescue of coronal suture because treated ERF$^{LoxP/-}$ mice have normal width compared to both treated and untreated ERF$^{LoxP/+}$, while untreated ERF$^{LoxP/-}$ mice present statistically

smaller width in their coronal sutures (*Figure 1c,1d, and 1e*). In the case of sagittal suture, all U0126-treated ERF$^{LoxP/-}$ mice manifest opened sagittal sutures, while untreated group has mainly closed sagittal suture. Despite the open state of suture in treated group, there is no statistical significance between the U0126-treated and untreated group of ERF$^{LoxP/-}$ mice (*Figure 1f & 1g*).

a

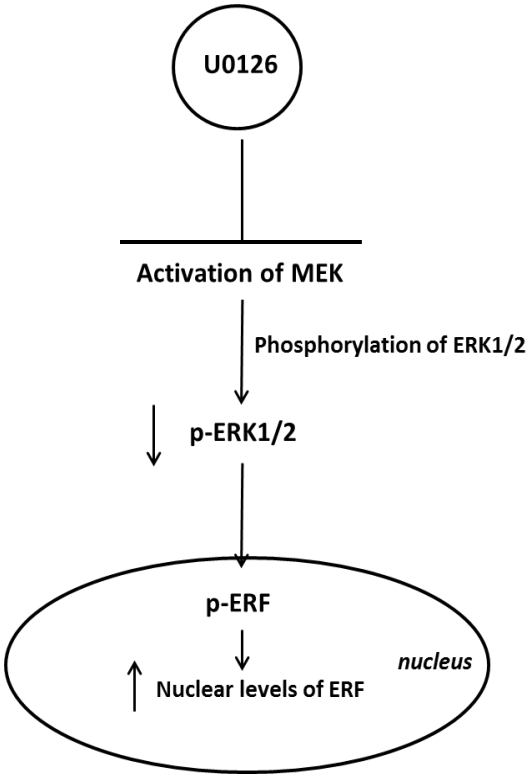

b

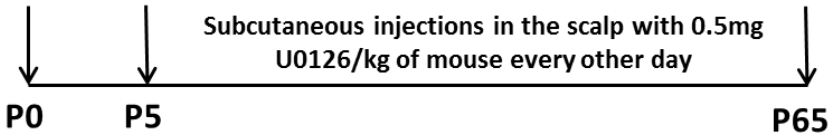

ERF LoxP/+ U0126	n=15	P65
ERF LoxP/- U0126	n=9	P65
ERF LoxP/+ DMSO	n=25	P63-P65
ERF LoxP/- DMSO	n=19	P63-P65

c

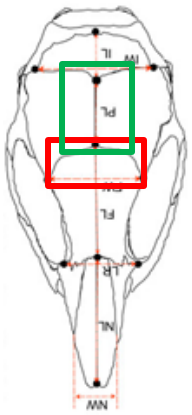

d

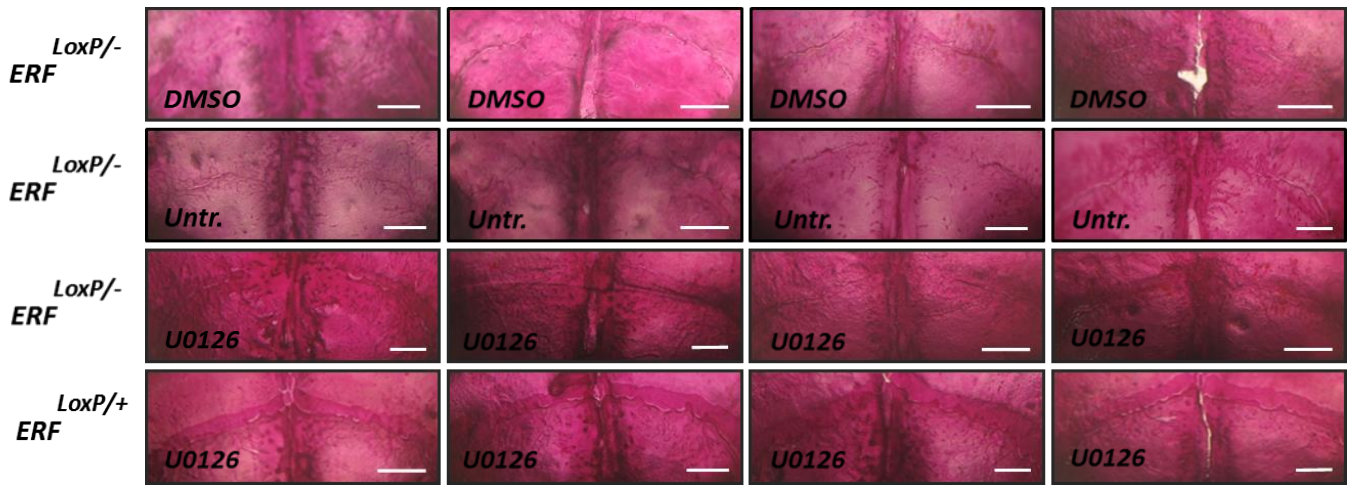

e

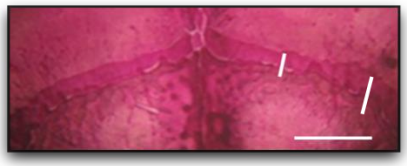

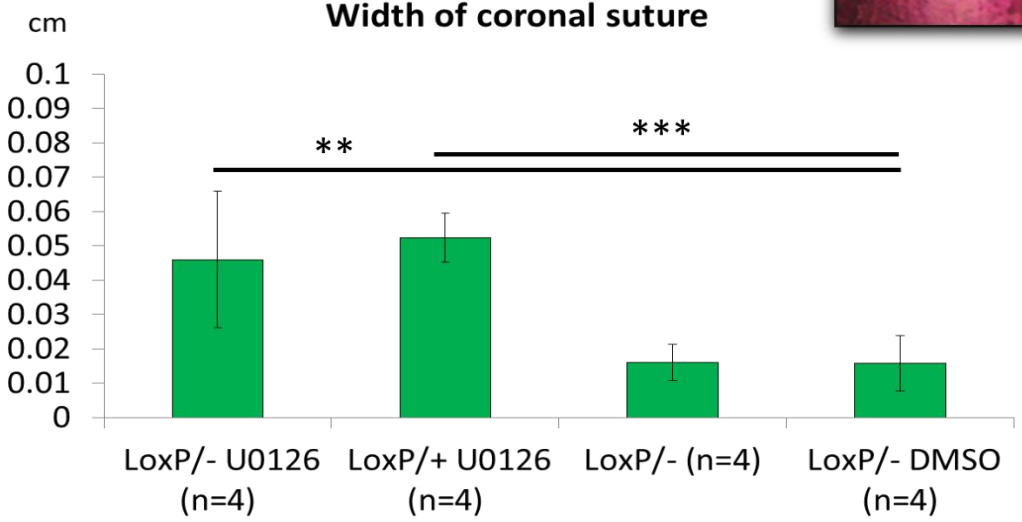
Width of coronal suture
cm
0.1
0.09
0.08
0.07
0.06
0.05
0.04
0.03
0.02
0.01
0
**
***
LoxP/- U0126 (n=4)
LoxP/+ U0126 (n=4)
LoxP/- (n=4)
LoxP/- DMSO (n=4)

f

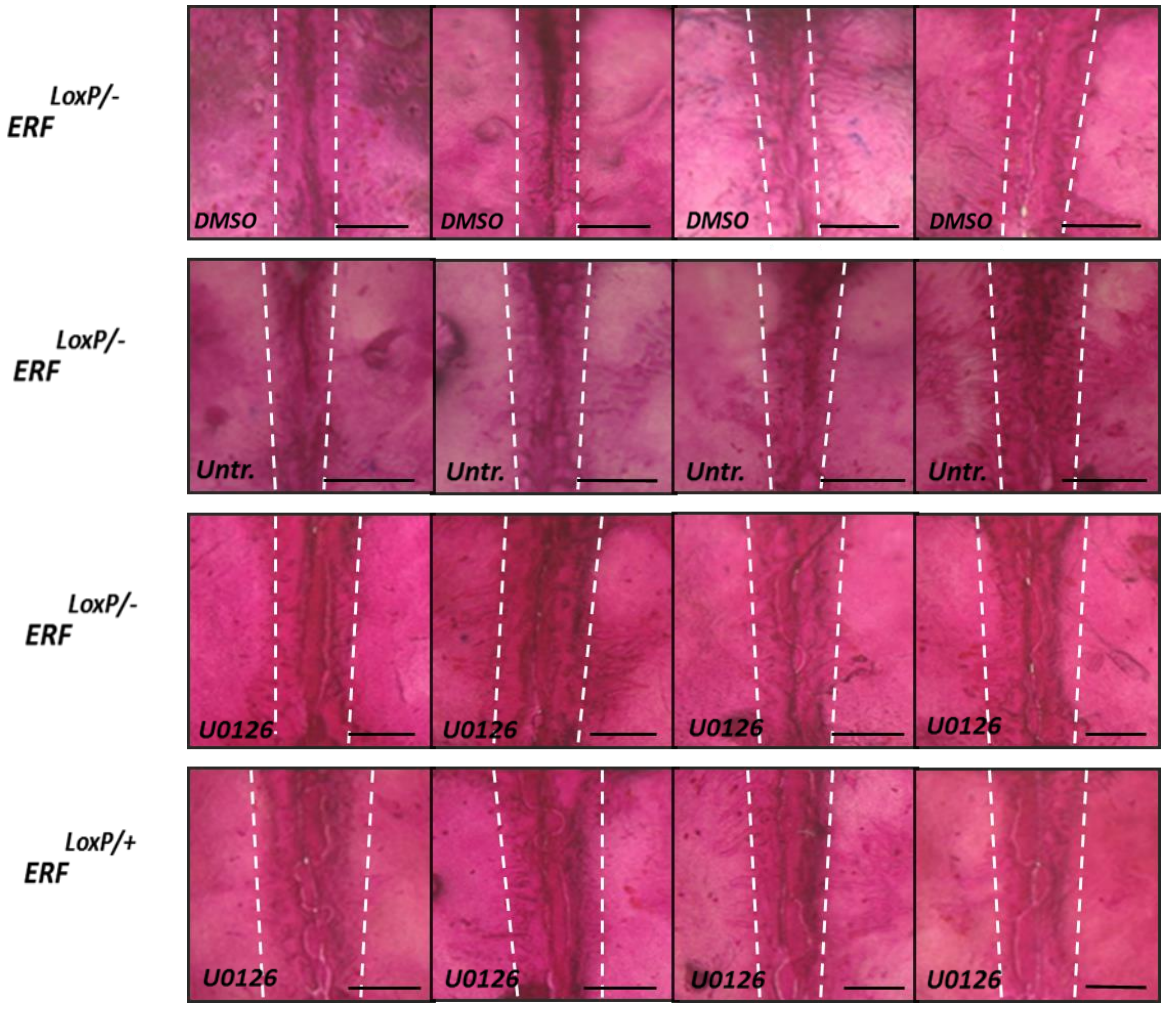
LoxP/- ERF
DMSO
LoxP/- ERF
Untr.
LoxP/- ERF
U0126
LoxP/+ ERF
U0126

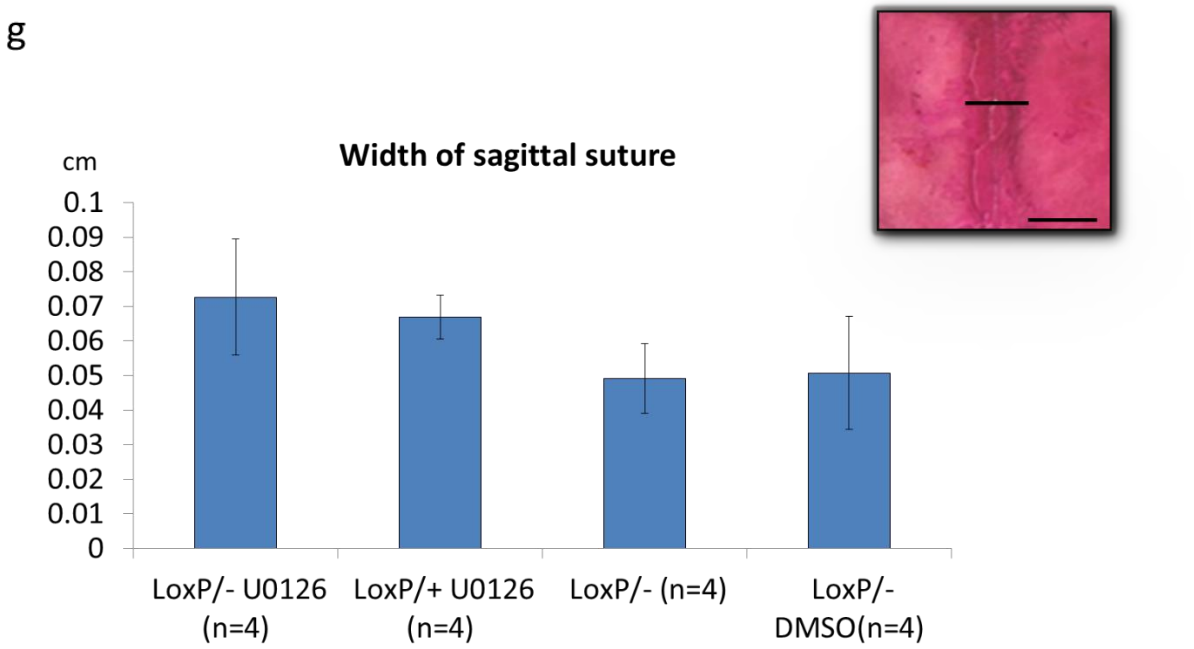

Figure 1. Subcutaneous administration of U0126 rescues the suture closure in the cranial vault of ERF$^{LoxP/-}$ mice. (a) Schematic representation of U0126 effect in the MEK-ERK-ERF signaling. **(b)** Workflow of subcutaneous administrations and final numbers of treated and untreated groups. **(c)** Schematic representation of the skull with the cranial sutures. **(d)** Staining of skulls with Alcian Blue & Alizarin Red S staining for all groups and focused snapshots of coronal sutures, showing opened coronal sutures in the case of treated ERF$^{LoxP/-}$ mice versus untreated group. Scale bars, 1 mm. **(e)** Quantification of coronal suture width has shown opened coronal sutures in the majority of mice upon exposure to U0126. **(f)** Focused snapshots in sagittal sutures of stained skulls, showing that U0126-treated have opened sagittal suture. Scale bar, 1 mm. **(e)** Quantification of sagittal suture width has shown increase in the width of ERF$^{LoxP/-}$ mice but no statistical significance between the treated and untreated groups. In all charts, error bars represent the s. d. In all panels, statistical significance was determined with one-way ANOVA and Bonferroni post-hoc t tests. $^{**}P<0.01$, $^{***}P<0.001$.

Subcutaneous administration of KPT-330 in ERF$^{LoxP/-}$ mice

Based on the aforementioned data about ERF-complex craniosynostosis, another potential therapeutic approach is the nuclear accumulation of ERF. For this reason, use of a selective inhibitor of nuclear exportin XPO1 KPT-330 is another strategy in order to alleviate the ERF-related craniosynostosis phenotypical defects. The blockage of ERF in the nucleus has the aim of accumulating this factor and forcing it to play its osteogenic role in the suture patency program (Figure 2a). Preliminary data using GFP-ERF construct and the KPT-330 have shown that this inhibitor can block the export of fusion ERF and subsequently of endogenous ERF (unpublished data). Furthermore, intraperitoneal administration from postnatal day 5th until 25th has shown some corrections in the facial phenotypical traits of ERF$^{LoxP/-}$ mice (unpublished data). Using the same protocol of subcutaneous administrations with U0126, there are enough mice group that are completed and they are ready for the staining of Alcian Blue and Alizarin Red S staining (Figure 2b). Until now, it is impossible to come in any conclusion about the suture closure and the facial traits of KPT-330 subcutaneously treated mice.

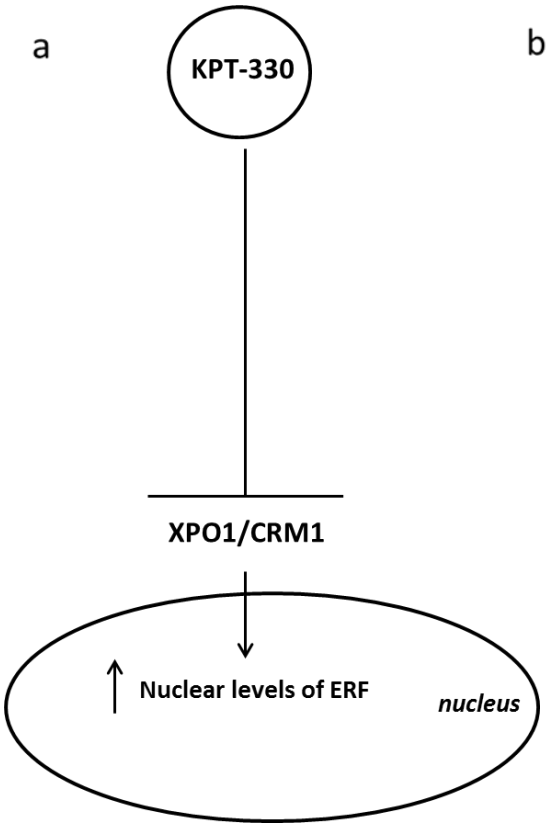

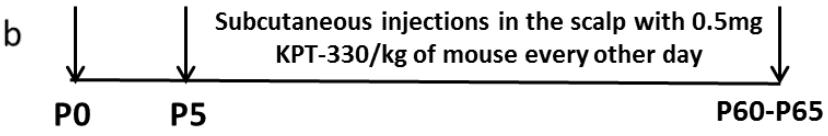

ERF LoxP/+ KPT-330	n=15	P60-P65
ERF LoxP/- KPT-330	n=11	P60-P65
ERF LoxP/+ DMSO	n=25	P63-P65
ERF LoxP/- DMSO	n=19	P63-P65

Figure 2. Subcutaneous administration of KPT-330 in the cranial vault of ERF$^{LoxP/-}$ mice. (a) Schematic representation of KPT-330 effect in ERF localization. **(b)** Workflow of subcutaneous administration of KPT-330 and final number of treated and untreated mice groups.

Studying the overall growth of ERF$^{LoxP/-}$ mice upon exposure to U0126

Based on previous evidence, MEK inhibitor is potentially a drug for the rescue of growth retardation in Apert mouse syndrome and Noonan syndrome.[67],[68] So, subcutaneous administration of MEK inhibitor in ERF$^{LoxP/-}$ and ERF$^{LoxP/+}$ every other day and sacrifice of mice approximately in postnatal day 65th (9th week of their life) permits the overall evaluation of their growth upon their exposure in MEK inhibitor. Compared to the control group of ERF$^{LoxP/-}$ mice, U0126 treated mice present a moderate increase in their size. Furthermore, untreated ERF$^{LoxP/-}$ present statistical differences both in treated and untreated ERF$^{LoxP/+}$, while these differences are not existed for treated group. So, U0126 seems to correct the overall growth of ERF$^{LoxP/-}$ mice, but it is necessary the increase of their mice for reassuring the observed difference.

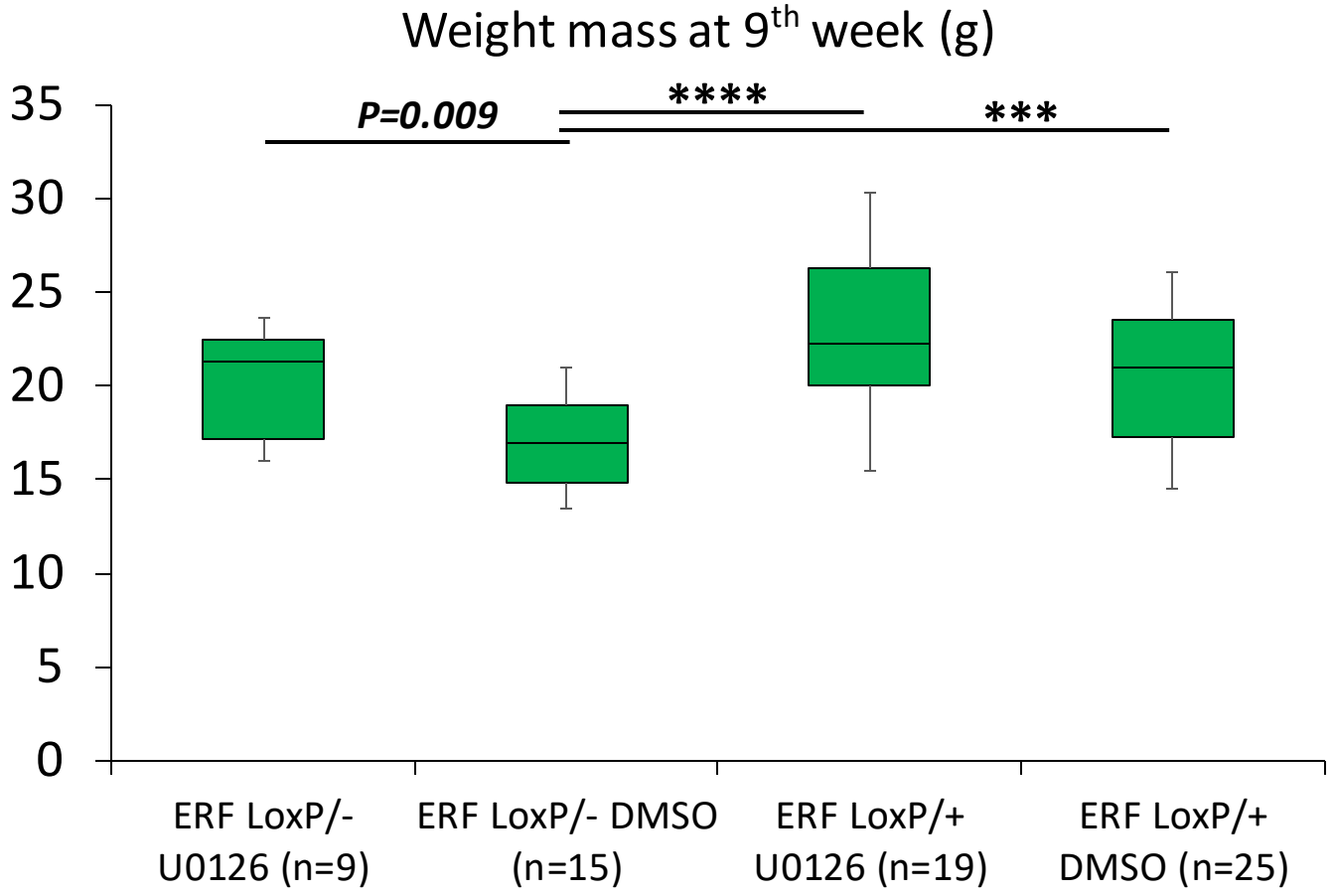

Figure 3. Effect of U0126 in the overall growth of ERF$^{LoxP/-}$ mice. U0126-treated group seems to have more normal final growth compared to untreated group. Statistical significance was determined using one-way ANOVA and Bonferroni post-hoc t test. ***P<0.001, ****P<0.0001.

Studying the overall growth of ERF$^{LoxP/-}$ mice upon exposure to KPT-330

KPT-330 is a blocker of XPO1 and it has been used for various malignant cancers.[59],[60] It is the first time that this inhibitor was used for the treatment of a craniofacial disease. Compared to the untreated group, KPT-330 subcutaneous administration does not change the overall growth of ERF$^{LoxP/-}$ mice, while it does not affect the overall growth of ERF$^{LoxP/+}$ mice. Consequently, KPT-330 inhibitor is unable to improve the overall developmental program of ERF$^{LoxP/-}$ mice. Also, the administered dosage is not toxic for the mice.

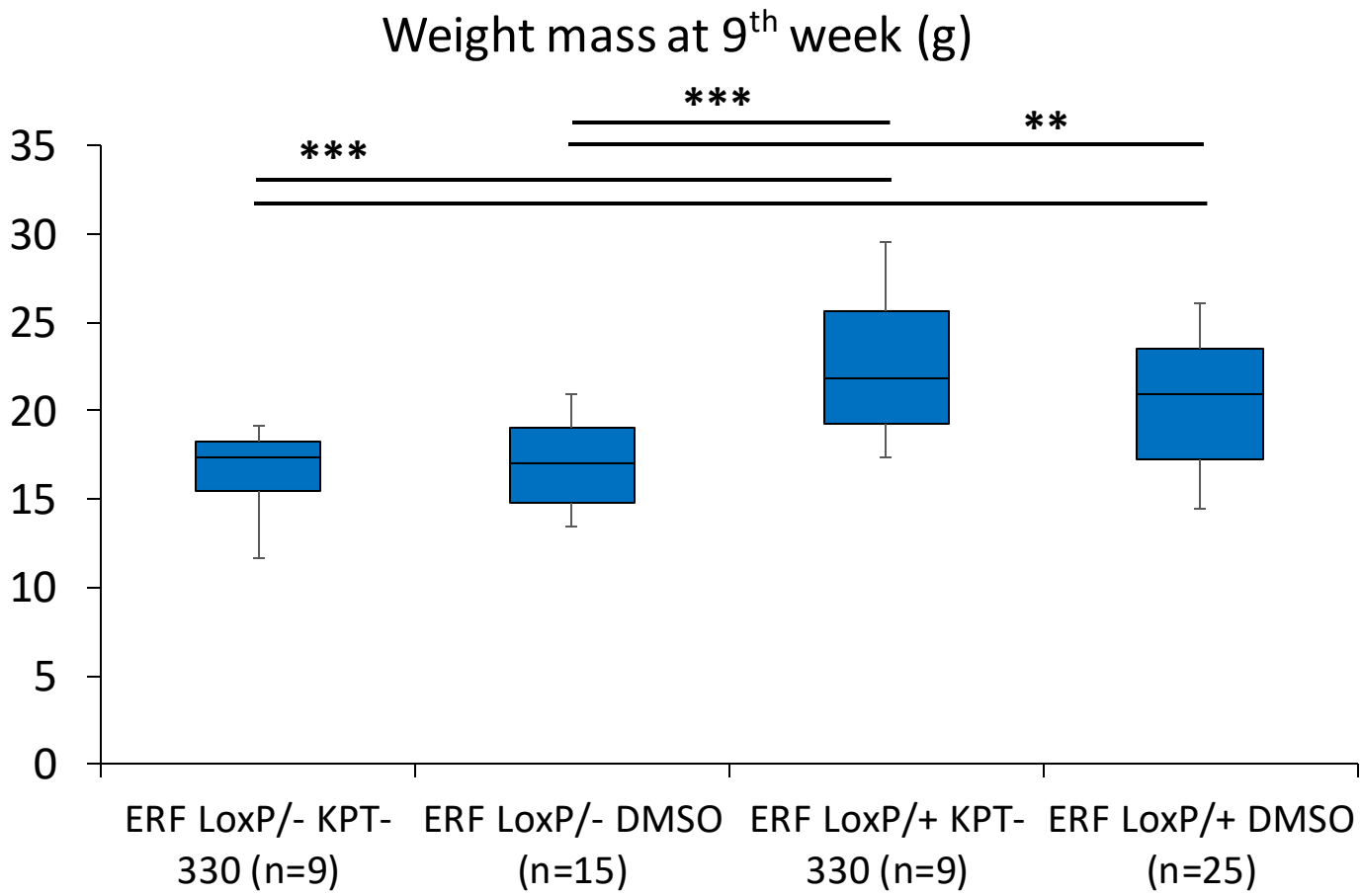

Figure 4. Effect of KPT-330 in the overall growth of ERF$^{LoxP/-}$ mice. KPT-330 does not improve the overall growth of treated group versus to untreated group. Statistical significance was determined using one-way ANOVA and Bonferroni post-hoc t test. ***P*<0.01, ****P*<0.001.

Proving the change of ERK-ERF signaling upon U0126 exposure and the presence of MEK inhibitor into the bloodstream

Doing the subcutaneous injections in mice, it is necessary for the support of the previous results the proof that this type of administration is ideal as treatment for the craniosynostosis disease. For this reason, subcutaneous injections with U0126 in the cranial vault of a B6 mouse was done. In a similar way, a subcutaneous injection with the vehicle (1:1) DMSO/PBS 1X was done in the cranial vault of another B6 mouse. Moreover, as positive control was used a mouse that was injected intraperitoneally with 10x more concentrated dosage of U0126. After the time passage of 6 hours, protein extraction from the cranial vault of the three mice showed that the two different administrations of U0126 reduced the overall p-ERK1/2 levels compared to the untreated mouse (Figure 5a & 5b). Quantification of the observed signals of the different proteins indicates that control mouse has 2-3 more p-ERK1/2 levels compared to the U0126-treated mice. However, a repetition of this experiment will enhance the observed difference between the treated and untreated situations. Simultaneously, after the time passage of 2 and 6 hours, the collection of mouse blood, isolation of plasma and their incubation in GFP-ERF transfected HeLa cells causes a slight increase both in ubiquitous and nuclear signal of GFP-ERF (Figure 5c & 5d). Compared to the control condition, the extracted plasma, coming from U0126-intraperitoneally injected mice, might contain some quantity of the drug, capable of reducing the number of cytoplasmic signal of GFP-ERF. Consequently,

U0126 probably is circulating in the bloodstream, in the case of the intraperitoneal injection, as a result, this administration causes the systematic circulation of this inhibitor. In the case of subcutaneous administration, probably the dosage is consumed by the local tissue/cranial vault.

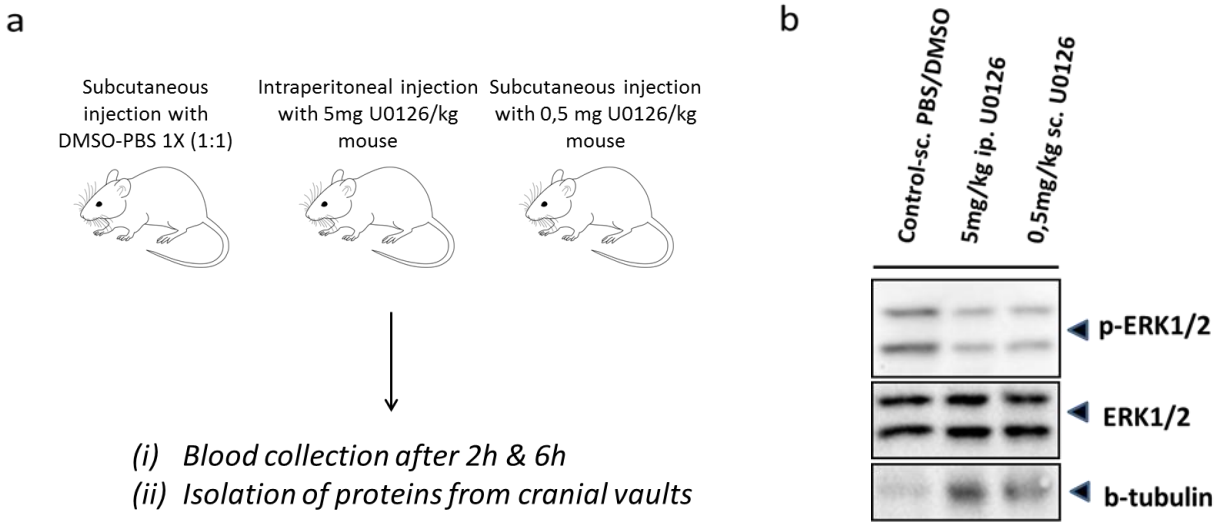

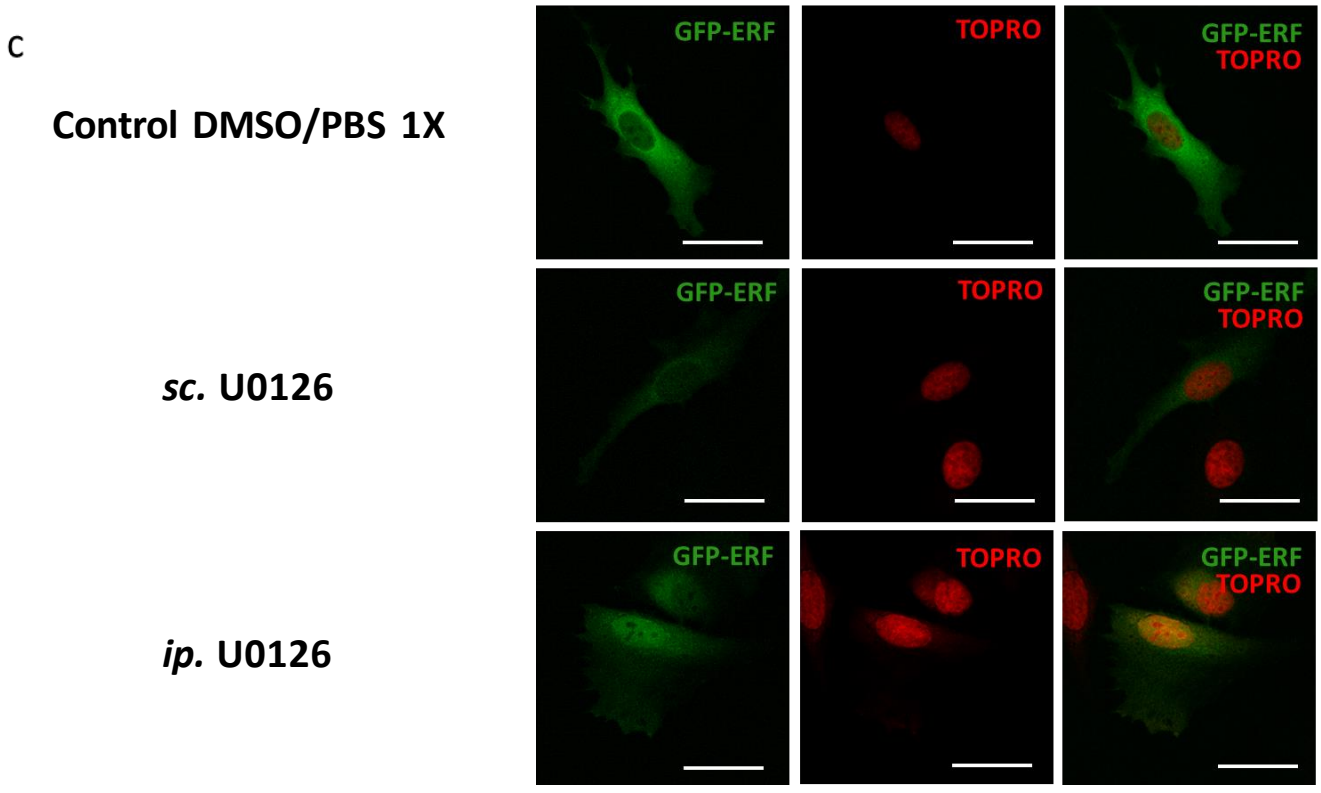

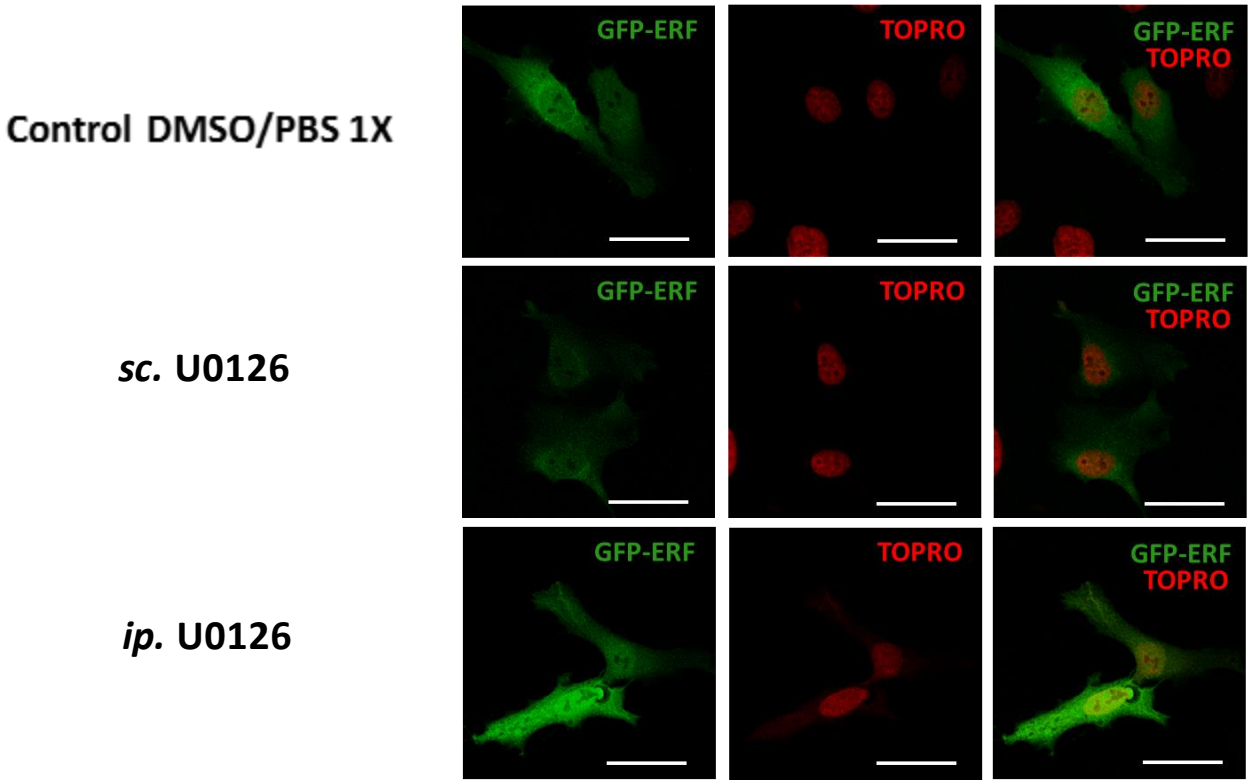
Control DMSO/PBS 1X
sc. U0126
ip. U0126
GFP-ERF
TOPRO
GFP-ERF
TOPRO

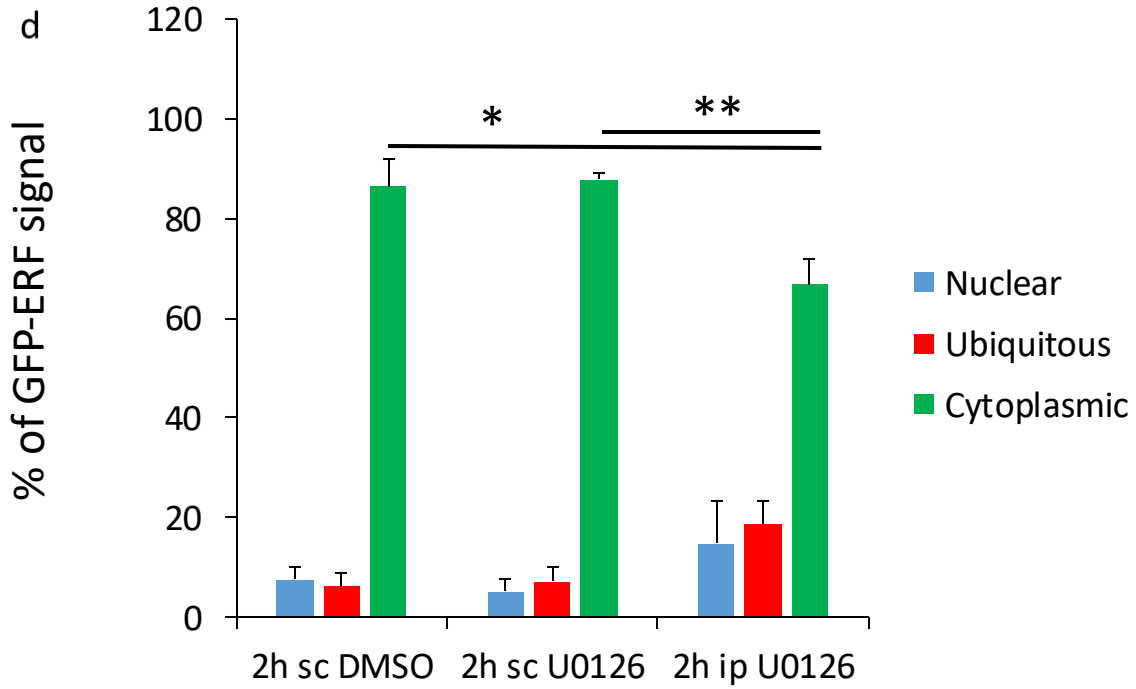
d
% of GFP-ERF signal
120
100
80
60
40
20
0
*
**
2h sc DMSO
2h sc U0126
2h ip U0126
Nuclear
Ubiquitous
Cytoplasmic

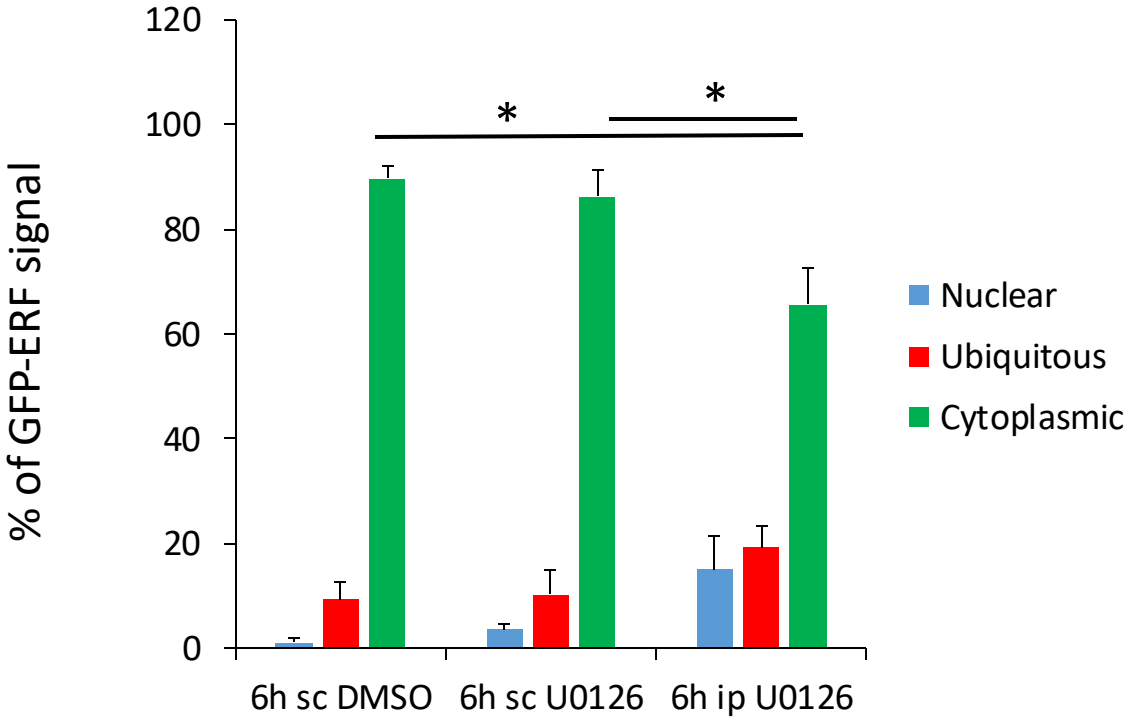
120
100
80
60
40
20
0
% of GFP-ERF signal
*
*
Nuclear
Ubiquitous
Cytoplasmic
6h sc DMSO
6h sc U0126
6h ip U0126

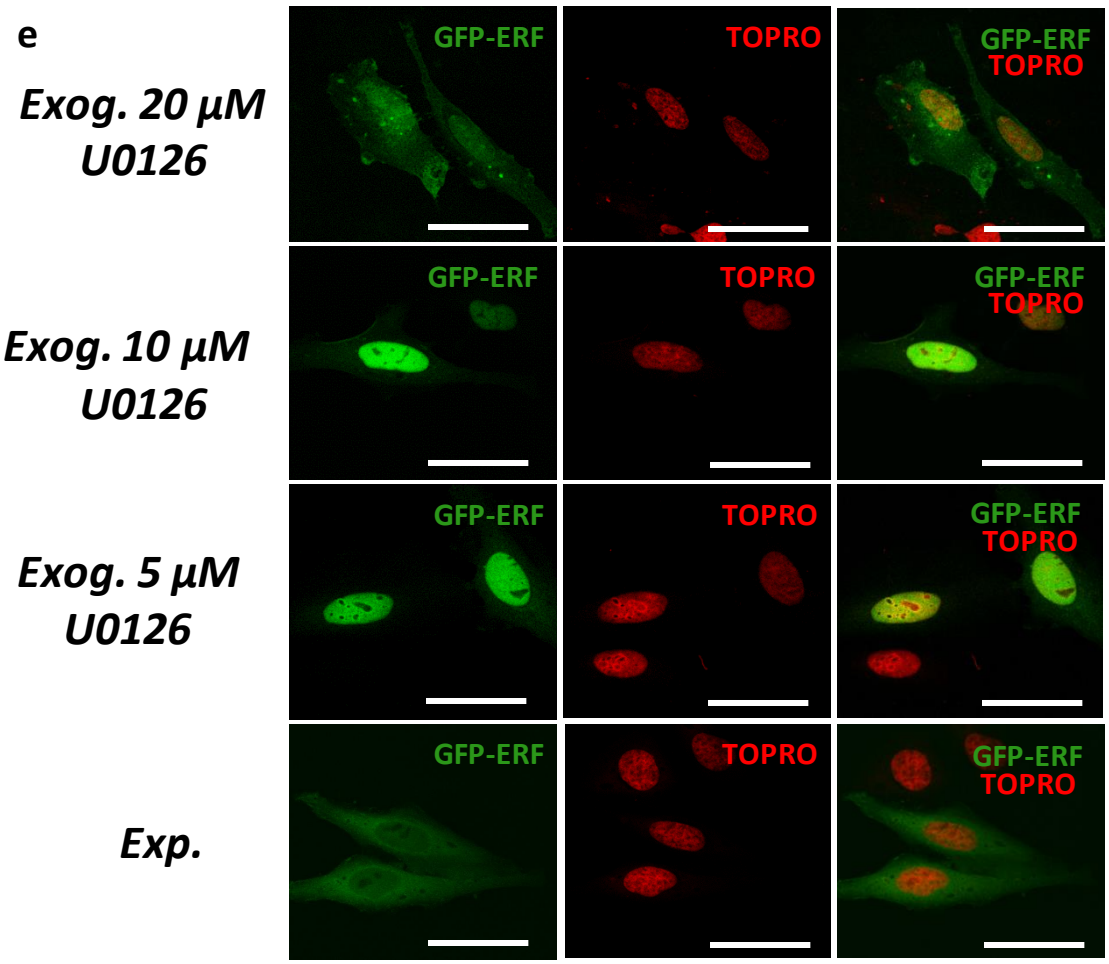
e
Exog. 20 µM U0126
Exog. 10 µM U0126
Exog. 5 µM U0126
Exp.
GFP-ERF
TOPRO
GFP-ERF TOPRO

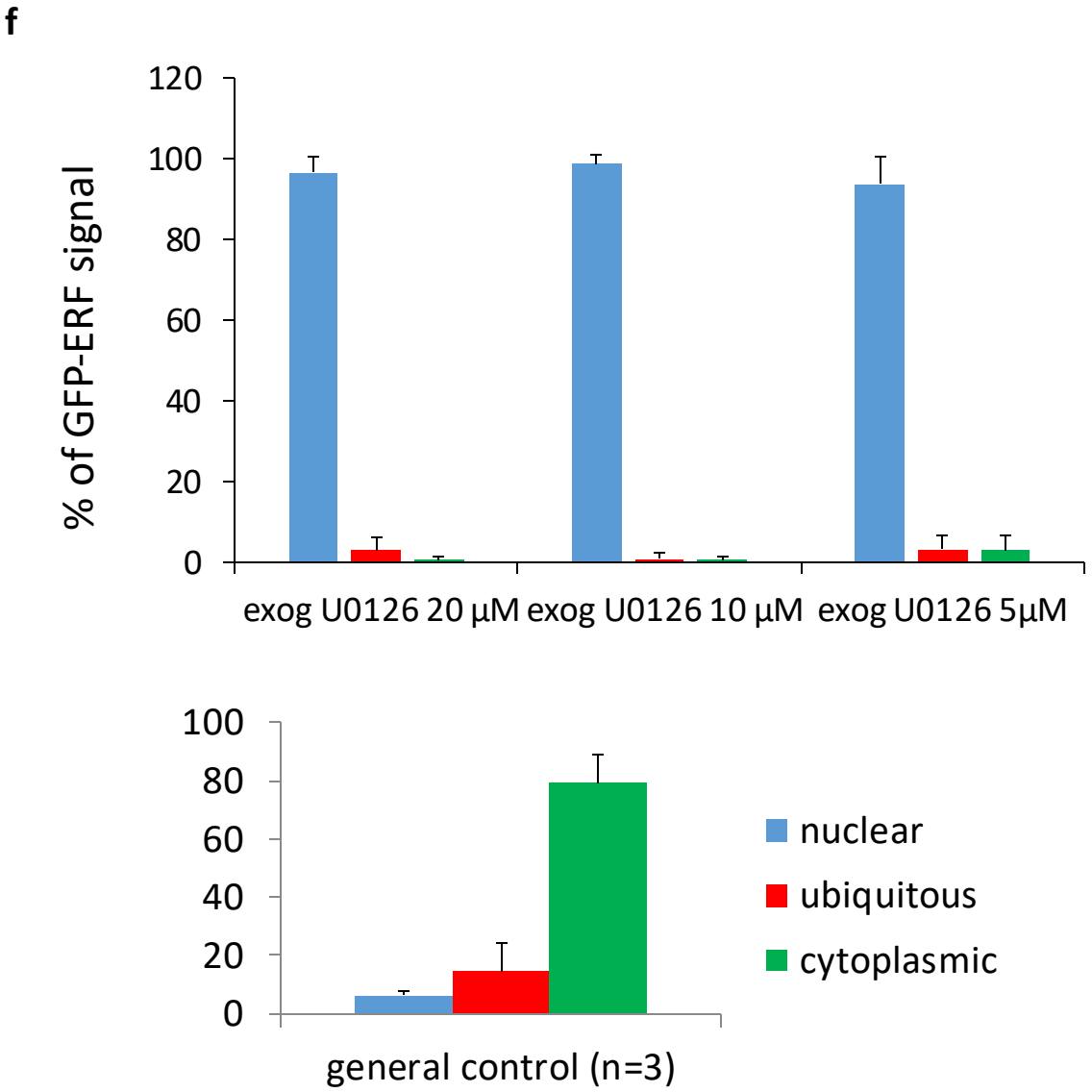

Figure 5. Administration of U0126 reduces the activated ERK1/2 levels in the mouse cranial vault. **(a)** Schematic representation of workflow, **(b)** Western blot shows that two different administrations with U0126 reduce the p-ERK1/2 levels compared to the control mouse. **(c)** Representative images from the incubated GFP-ERF HeLa cells with the extracted mouse bloods, showing a slight increase in both the ubiquitous and nuclear signal. Scale bars, 50µm. **(d)** Quantification of GFP-ERF localization on HeLa cells shows that U0126 inhibitor is probably circulated into the bloodstream. **(e & f)** Positive control adding exogenously MEK inhibitor and exponential condition of GFP-ERF transfected HeLa cells as negative control. For each condition was measured 50 cells. Statistical significance was determined using two-tailed t test. **P*<0.05, ***P*<0.01.

Discussion

Based on the previous pharmacological approaches, regulation of ERF localization in ERF$^{LoxP/-}$ mice is critical for the alleviation of craniosynostosis phenotype defects. Subcutaneous administration of MEK inhibitor U0126 not only corrects the sagittal and coronal suture, but also seems to improve the overall growth of

$ERF^{LoxP/-}$ mice. However, separation between males and females, as well as more mice can give further elucidation for the improvement of their growth retardation trait. Compared to the intraperitoneal administration, there are evidence for the effect of U0126 through subcutaneous administrations in the cranial vault in WT B6 mice and this type of administration gives detectable levels of this inhibitor in the bloodstream. In the case of SINE KPT-330, treated mice are under the staining procedure, but it has been observed after the sacrifice of some mice, the moderately opened coronal and sagittal suture. Relevant to their growth, KPT-330 does not appear to increase their overall size in $ERF^{LoxP/-}$ mice. Finally, there are evidence that subcutaneous administration of both inhibitors does not lead to their systematic circulation in mice, while in intraperitoneal administration this effect is inevitable. The final assessment of the cranial bones and the suture closure will be accomplished through the μCT scanning, which is the most objective way of analyzing and measuring bone morphometrics.

Afterwards, the next step for the elucidation of the molecular pathways in ERF-complex craniosynostosis will be the exposure of cells and mice in each inhibitor, separately. Given the fact that osteogenesis is affected by many different pathways, such as BMP, TGF-b, MAPK, FGF and Hedgehog signaling, it would be interesting to extract RNA and proteins from both treated and untreated $ERF^{LoxP/-}$, as well treated and untreated $ERF^{LoxP/+}$ mice. Until now, knowing that FGF2 contributes to the enhancement of craniosynostosis phenotype, and also, ERF is a negative regulator of FGF2 in the placenta, it would be important to distinguish the regulation of FGF-2 by ERF, in craniosynostosis.[23],[24] Furthermore, treatment with FGF2 accelerates the closure of sutures in ex vivo cultures, making it an interesting candidate for the regulation of suture patency.[74] Probably, use of both SINE and MEK inhibitors in vitro culture of suture cells can answer in the change of regulation of FGF2 due to the nuclear accumulation of ERF.

Based on the context of ERF in the cancer, it is known that this factor, through suppression of Sema-7a, blocks the EMT process, blocking the cancer progression.[27] In the case of skull morphogenesis, migration of mesenchymal stem cells and more differentiating osteoblasts migrate from the sutures to frontal or parietal bones for the right expansion of the skull.[75],[77],[79] In the case of EMT, levels of Snail and Slug are not affected by the ERF function.[27] However, its absence of these facilitators of EMT in skeletal stem cells can lead to defective skull morphogenesis and long bone defects.[84] For this reason, it would be interesting to check the regulation of Snail/Slug and Sema-7a in the migration of suture cells in the expanding osteogenic fronts. Checking these factors, it will be excluded the fact that ERF-complex craniosynostosis is a disease, caused by defective migration of suture stem cells. Moreover, Snail/Slug are regulators of skeletal stem cell renewal, differentiation and bone formation.[84] So, if these factors are expressed in reduced or increased levels of due to the absence of ERF inside the nucleus, then it would be more prominent the molecular mechanism of ERF in the post-natal program of skull morphogenesis.

Finally, in the case of protein extracts, dissecting specific regions of the mouse skulls, (such as sagittal, coronal, lamboid, frontal, parietal, and nose) will be assessed if the crosstalk between the different osteogenesis-related pathways in $ERF^{LoxP/-}$ is normal and their exposure in the inhibitors changes some specific signaling. The ideal proof for the change of signaling in the context of osteogenesis will be the cryosections of treated and untreated mice and their immunostaining in order to see in single cell analysis the changes of the osteogenesis pathways. Moreover, another way of dissecting the role of ERF in osteogenesis will be the RNA extraction of mouse skull regions and the use of RT-PCR for FGF-responsive and other genes, indicative for the activation/suppression of each pathway in the context of osteogenesis. Especially, in the case of Dusp and Sprouty genes, chip-seq data in starvated condition in MEFs have shown that ERF binds in the majority of them. Consequently, it would be interesting to see if ERF has regulatory role in these FGF-responsive genes. Using either the MEK inhibitor or the SINE KPT-330 for the nuclear

accumulation of ERF it would be interesting to check the response of ERF in their switch on/off of these genes, improving this auto-feedback loop of FGFR signaling. The validation of these results for the switch on-off of the genes in the case of their promoters or enhancers, will be completed using luc-assays for the enhancement of the research findings. Finally, it would be interesting for the case of KPT-330 inhibitor to prove that the sustained nuclear accumulation of p-ERF can cause the dephosphorylation of this protein and it's binding to the genome. Probably, the blocking of XPO1 can cause the accumulation of a phosphatase, which is capable of dephosphorylating the ERF.

References

[1] Oikawa, T., & Yamada, T. (2003). Molecular biology of the Ets family of transcription factors. *Oncogene*, *303*, 11–34.

[2] Sementchenko, V. I., & Watson, D. K. (2000). Ets target genes : past, present and future.

[3] Raouf, A., & Seth, A. (2000). Ets transcription factors and targets in osteogenesis. *Oncogene*, *19*(55), 6455–6463.

[4] Trojanowska, M. (2000). Ets factors and regulation of the extracellular matrix. *Oncogene*, 6464–6471.

[5] Leprince, D., Gegonne, A., Coll, J., de Taisne, C., Schneeberger, A., Stehelin, D. (1983). A putative second cell-derived oncogene of avian leukaemia retrovirus E26. *Nature*, 306, 395–397.

[6] Karim F.D., Urness L.D., Thummel C.S., Klemsz M.J., McKercher S.R., Celada A., Van Beveren C., Maki R.A., Gunther C.V., Nye J.A. and et al. (1990). *Genes Dev*., 4, 1451-1453.

[7] Graves, B. J., & Petersen, J. M. (1998). Specificity within the ets Family of Transcription Factors. *Advances in Cancer Research*, *75*, 1–57.

[8] Kim, C.A., Phillips, M.L., Kim, W., Gingery, M., Tran, H.H., Robinson, M.A., Faham, S., Bowie, J.U., (2001). Polymerization of the SAM domain of TEL in leukemogenesis and transcriptional repression. *EMBO J.* 20, 4173–4182.

[9] Kodandapani, R., (1996). A new pattern for helix–turn–helix recognition revealed by the PU.1 ETS domain DNA complex. *Nature*. 380, 456–460.

[10] Donaldson, L.W., Petersen, J.M., Graves, B.J., McIntosh, L.P., 1996. Solution structure of the ETS domain from murine Ets-1: a winged helix-turn-helix DNA binding motif. *EMBO J.* 15, 125–134.

[11] Ghysdael J and Boureux A. (1997). The ETS family of transcriptional regulators. In: Oncogenes as Transcriptional Regulators, M Yaniv and J Ghysdael, (eds). Vol. 1 Birkhauser Verlag: Basel, Switzerland, pp. 29-88.

[12] Le Gallic, L., Sgouras, D., Beal, G., & Mavrothalassitis, G. (1999). Transcriptional repressor ERF is a Ras/mitogen-activated protein kinase target that regulates cellular proliferation. *Molecular and Cellular Biology*, *19*(6), 4121–33.

[13] Rabault, B., & Ghysdael, J. (1994). Calcium-induced phosphorylation of ETS1 inhibits its specific DNA binding activity. *Journal of Biological Chemistry*, *269*(45), 28143–28151.

[14] Marais, R., Wynne, J., & Treisman, R. (1993). The SRF accessory protein Elk-1 contains a growth factor-regulated transcriptional activation domain. *Cell*, *73*(2), 381–393.

[15] Dalton S and Treisman R (1992) Characterization of SAP-1, a protein recruited by *serum response factor to the c-fos serum response element. Cell, 68 (3): 597-612.*

[16] Mavrothalassitis, G., & Ghysdael, J. (2000). Proteins of the ETS family with transcriptional repressor activity. *Oncogene*, *19*, 6524–6532.

[17] Sgouras, D. N., Athanasioul, M. a, Beal, G. J., Fisherl, R. J., Blair, D. G., & Mavrothalassitis, G. J. (1995). Phosphorylation during Cell Cycle and Mitogenic Stimulation, *14*(19), 4781–4793.

[18] Mavrothalassitis, G. J., & Papas, T. S. (1991). Positive and negative factors regulate the transcription of the ETS2 gene via an oncogene-responsive-like unit within the ETS2 promoter region. *Cell Growth & Differentiation: The Molecular Biology Journal of the American Association for Cancer Research*, *2*, 215–224.

[19] Le Gallic, L., Sgouras, D., Beal, G., & Mavrothalassitis, G. (1999). Transcriptional repressor ERF is a Ras/mitogen-activated protein kinase target that regulates cellular proliferation. *Molecular and Cellular Biology*, *19*, 4121–4133.

[20] Polychronopoulos, S., Verykokakis, M., Yazicioglu, M. N., Sakarellos-Daitsiotis, M., Cobb, M. H., & Mavrothalassitis, G. (2006). The transcriptional ETS2 repressor factor associates with active and inactive Erks through distinct FXF motifs. *Journal of Biological Chemistry*, *281*, 25601–25611.

[21] Le Gallic, L., Virgilio, L., Cohen, P., Biteau, B., & Mavrothalassitis, G. (2004). ERF nuclear shuttling, a continuous monitor of Erk activity that links it to cell cycle progression. *Molecular and Cellular Biology*, *24*, 1206–1218.

[22] Verykokakis, M., Papadaki, C., Vorgia, E., Le Gallic, L., & Mavrothalassitis, G. (2007). The RAS-dependent ERF control of cell proliferation and differentiation is mediated by c-Myc repression. *Journal of Biological Chemistry*, *282*(41), 30285–30294.

[23] Papadaki, C., Alexiou, M., Cecena, G., Verykokakis, M., Bilitou, A., Cross, J. C.,… Mavrothalassitis, G. (2007). Transcriptional repressor erf determines extraembryonic ectoderm differentiation. *Molecular and Cellular Biology*, *27*(14), 5201–5213.

[24] Vorgia, E., Zaragkoulias, A., Peraki, I., & Mavrothalassitis, G. (2017). Suppression of Fgf2 by ETS2 repressor factor (ERF) is required for chorionic trophoblast differentiation, (January), 1–10.

[25] Peraki I., Palis J., & Mavrothalassitis, G. (2017). The Ets2 repressor factor (ERF) is required for effective primitive and definitive hematopoiesis. Mol. Cell Biol. 2017 Jul 10. (00183-17).

[26] Twigg, S. R. F., Vorgia, E., Mcgowan, S. J., Peraki, I., Aimée, L., Mohammed, S. N.,… Wilson, L. C. (2013). Reduced dosage of ERF causes complex craniosynostosis in humans and mice, and links ERK1 / 2 signaling to regulation of osteogenesis. *Nature Genetics, 45*(3), 308–313.

[27] Allegra, M., et al. (2012). "Semaphorin-7a reverses the ERF-induced inhibition of EMT in Ras-dependent mouse mammary epithelial cells." Molecular Biology of the Cell **23**(19): 3873-3881.

[28] Huang, F. W., et al. (2017). "Exome Sequencing of African-American Prostate Cancer Reveals Loss-of-Function ERF Mutations." Cancer Discov. ; 7(9), 1-11.

[29] Bose, R., et al. (2017). "ERF mutations reveal a balance of ETS factors controlling prostate oncogenesis." Nature; **546**(7660): 671-675.

[30] Adachi Y, Yanagida M. (1989). Higher order chromosome structure is affected by cold-sensitive mutations in a Schizosaccharomyces pombe gene crm1+ which encodes a 115-kD protein preferentially localized in the nucleus and at its periphery. J Cell Biol.; 108: 1195–207.

[31] Fornerod M, Ohno M, Yoshida M, Mattaj IW. CRM1 is an export receptor for leucine-rich nuclear export signals. (1990). Cell; 90: 1051–60.

[32] Fukuda M, Asano S, Nakamura T, Adachi M, Yoshida M, Nishida E. (1997) CRM1 is responsible for intracellular transport mediated by the nuclear export signal. Nature. 390: 308–11.

[33] Ossareh-Nazari B, Bachelerie FO, Dargemont C. (1997). Evidence for a role of CRM1 in signal-mediated nuclear protein export. Science; 278: 141–4.

[34] Gravina, G. L., Mancini, A., Sanita, P., Vitale, F., Marampon, F., Ventura, L.,.. Festuccia, C. (2015). KPT-330, a potent and selective exportin-1 (XPO-1) inhibitor, shows antitumor effects modulating the expression of cyclin D1 and survivin in prostate cancer models. *BMC Cancer*, 1–19.

[35] Camus, V., Miloudi, H., Taly, A., & Sola, B. (2017). XPO1 in B cell hematological malignancies : from recurrent somatic mutations to targeted therapy, 1–13.

[36] Green, A. L., Ramkissoon, S. H., Mccauley, D., Jones, K., Perry, J. A., Hsu, J. H., … Kung, A. L. (2015). Neuro-Oncology, *17*(April 2014), 697–707.

[37] Parikh, K., Cang, S., Sekhri, A., & Liu, D. (2014). Selective inhibitors of nuclear export (SINE) – a novel class of anti-cancer agents, *330*, 1–8.

[38] Ishizawa J, Kojima K, Hail Jr N, Tabe Y, Andreeff M. (2015). Expression, function, and targeting of the nuclear exporter chromosome region maintenance 1(CRM1) protein. Pharmacol Ther.; 153:25–35.

[39] Newlands ES, Rustin GJ, Brampton MH. (1996). Phase I trial of elactocin. Br J Cancer; 74: 648-9.

[40] Wolff, B., Sanglier, J. J., & Wang, Y. (1997). Leptomycin B is an inhibitor of nuclear export: inhibition of nucleo-cytoplasmic translocation of the human immunodeficiency virus type 1 (HIV-1) Rev protein and Rev-dependent mRNA. *Chemistry & Biology*, *4*, 139–147.

[41] Kudo, N., Wolff, B., Sekimoto, T., Schreiner, E. P., Yoneda, Y., Yanagida, M.,… Yoshida, M. (1998). Leptomycin B inhibition of signal-mediated nuclear export by direct binding to CRM1. *Experimental Cell Research*, *242*, 540–547.

[42] Mutka, S. C., Yang, W. Q., Dong, S. D., Ward, S. L., Craig, D. A., Timmermans, P. B. M. W. M., & Murli, S. (2009). Identification of nuclear export inhibitors with potent anticancer activity in vivo. *Cancer Research*, *69*, 510–517.

[43] Saito N, Matsuura Y. (2013). A 2.1-A-resolution crystal structure of unliganded CRM1 reveals the mechanism of autoinhibition. Journal of molecular biology; 425:350–64.

[44] Monecke T, Haselbach D, Voss B, Russek A, Neumann P, Thomson E, et al. Structural basis for cooperativity of CRM1 export complex formation. (2013). Proceedings of the National Academy of Sciences of the United States of America; 110:960–5.

[45] Dian C, Bernaudat F, Langer K, Oliva MF, Fornerod M, Schoehn G, et al. (2013). Structure of a truncation mutant of the nuclear export factor CRM1 provides insights into the auto-inhibitory role of its Cterminal helix. Structure; 21:1338–49.

[46] Yuh Min Chook, and Ho Yee Joyce Fung. (2015). Atomic basis of CRM1-cargo recognition, release and inhibition. *Semin Cancer Biol.*; *1*(214), 52–61.

[47] Turner, J. G., Dawson, J., & Sullivan, D. M. (2015). Nuclear export of proteins and drug resistance in cancer, *83*(8), 1021–1032.

[48] Makde RD, England JR, Yennawar HP, Tan S. (2010). Structure of RCC1 chromatin factor bound to the nucleosome core particle. Nature; 467:562–6.

[49] Nemergut ME, Mizzen CA, Stukenberg T, Allis CD, Macara IG. (2001). Chromatin docking and exchange activity enhancement of RCC1 by histones H2A and H2B. Science; 292:1540–3.

[50] Bischoff FR, Ponstingl H. (1991). Catalysis of guanine nucleotide exchange on Ran by the mitotic regulator RCC1. Nature; 354:80–2.

[51] Bischoff FR, Klebe C, Kretschmer J, Wittinghofer A, Ponstingl H. (1994). RanGAP1 induces GTPase activity of nuclear Ras-related Ran. Proceedings of the National Academy of Sciences of the United States of America; 91:2587–91.

[52] Hopper AK, Traglia HM, Dunst RW. (1990).The yeast RNA1 gene product necessary for RNA processing is located in the cytosol and apparently excluded from the nucleus. The Journal of cell biology; 111:309–21.

[53] Matunis MJ, Coutavas E, Blobel G. (1996). A novel ubiquitin-like modification modulates the partitioning of the Ran-GTPase-activating protein RanGAP1 between the cytosol and the nuclear pore complex. The Journal of cell biology; 135:1457–70.

[54] Lapalombella, R., Sun, Q., Williams, K., Tangeman, L., Jha, S., Zhong, Y.,… Byrd, J. C. (2012). Selective inhibitors of nuclear export show that CRM1/XPO1 is a target in chronic lymphocytic leukemia. *Blood*, *120*, 4621–4634.

[55] Xu D, Farmer A, Chook YM. (2010). Recognition of nuclear targeting signals by Karyopherin-β proteins. *Current opinion in structural biology*; 20(6):782-790.

[56] Dong, X., Biswas, A., Süel, K. E., Jackson, L. K., Martinez, R., Gu, H., & Chook, Y. M. (2009). Structural basis for leucine-rich nuclear export signal recognition by CRM1. *Nature*, *458*, 1136–1141.

[57] Monecke, T., Güttler, T., Neumann, P., Dickmanns, A., Görlich, D., & Ficner, R. (2009). Crystal structure of the nuclear export receptor CRM1 in complex with Snurportin1 and RanGTP. *Science (New York, N.Y.)*, *324*, 1087–1091.

[58] Güttler, T., Madl, T., Neumann, P., Deichsel, D., Corsini, L., Monecke, T.,… Görlich, D. (2010). NES consensus redefined by structures of PKI-type and Rev-type nuclear export signals bound to CRM1. *Nature Structural & Molecular Biology*, *17*, 1367–1376.

[59] Etchin J, Berezovskaya A, Conway AS, et al. (2017). KPT-8602, a second-generation inhibitor of XPO1-mediated nuclear export, is well tolerated and highly active against AML blasts and leukemia-initiating cells. *Leukemia*; 31 (1):143-150.

[60] Thomas Vercruysse, Jolien De Bie, Jasper E Neggers1, Maarten Jacquemyn, Els Vanstreels, Jonathan L Schmid-Burgk, Veit Hornung, Erkan Baloglu, Yosef Landesman5, William Senapedis, Sharon Shacham, Antonis Dagklis, Jan Cools, Dirk Daelemans. (2017).The second-generation exportin-1 inhibitor KPT-8602 demonstrates potent activity against acute lymphoblastic leukemia. *Clin Cancer Res*.; 15; 23 (10):2528-2541.

[61] Xu, L., Liu, Y., Hou, Y., & Wang, K. (2015). U0126 promotes osteogenesis of rat bone-marrow-derived mesenchymal stem cells by activating BMP / Smad signaling pathway, 537–545.

[62] Garrington TP, Johnson GL. (1999). Organization and regulation of mitogen-activated protein kinase signaling pathways. Curr. Opin. Cell Biol. 11:211–218.

[63] Fischmann, T. O., Smith, C. K., Mayhood, T. W., Myers, J. E., Reichert, P., Mannarino, A., … Madison, V. S. (2009). Crystal Structures of MEK1 Binary and Ternary Complexes with Nucleotides and Inhibitors, (D), 2661–2674.

[64] Robbins, D. J., Zhen, E., Owaki, H., Vanderbilt, C. A., Ebert, D., Geppert, T. D., and Cobb, M. H. (1993). Regulation and properties of extracellular signal-regulated protein kinases 1 and 2 in vitro. *J. Biol. Chem. 268*, 5097–5105.

[65] Schubbert, S., Shannon, K., & Bollag, G. (2007). Hyperactive Ras in developmental disorders and cancer, *7* (April), 295–308.

[66] Bentires-alj, M., Kontaridis, M. I., & Neel, B. G. (2006). Stops along the RAS pathway in human genetic disease, *12*(3), 283–285.

[67] Nakamura, T., Gulick, J., Pratt, R., & Robbins, J. (2009). Noonan syndrome is associated with enhanced pERK activity, the repression of which can prevent craniofacial malformations.

[68] Shukla, V., Coumoul, X., Wang, R., Kim, H., & Deng, C. (2007). RNA interference and inhibition of MEK-ERK signaling prevent abnormal skeletal phenotypes in a mouse model of craniosynostosis, *39*(9).

[69] Corson LB, Yamanaka Y, Lai KM, Rossant J. (2003). Spatial and temporal patterns of ERK signaling during mouse embryogenesis. *Development* 130:4527–4537.

[70] Jaiswal RK, Jaiswal N, Bruder SP, Mbalaviele G, Marshak DR, Pittenger MF. (2000). Adult human mesenchymal stem cell differentiation to the osteogenic or adipogenic lineage is regulated by mitogen activated protein kinase. J Biol Chem.; 275:9645–9652.

[71] Xiao G, Jiang D, Thomas P, Benson MD, Guan K, Karsenty G, Franceschi RT (2000) MAPK pathways activate and phosphorylate the osteoblast-specific transcription factor, Cbfa1. J Biol Chem.; 275: 4453–4459.

[72] Dang, Z., & Lowik, C. W. G. M. (2004). Differential Effects of PD98059 and U0126 on Osteogenesis and Adipogenesis, *533*, 525–533.

[73] Hotokezaka, H., Sakai, E., Kanaoka, K., Saito, K., Matsuo, K., Kitaura, H.,… Nakayama, K. (2002). U0126 and PD98059, Specific Inhibitors of MEK, Accelerate Differentiation of RAW264. 7 Cells into Osteoclast-like Cells *, *277*(49), 47366–47372.

[74] Morriss-Kay, G. M., & Wilkie, A. O. M. (2005). Growth of the normal skull vault and its alteration in craniosynostosis: insights from human genetics and experimental studies. *Journal of Anatomy*, *207*, 637–653.

[75] Jiang, X., Iseki, S., Maxson, R. E., Sucov, H. M., & Morriss-kay, G. M. (2002). Tissue Origins and Interactions in the Mammalian Skull Vault, *116*, 106–116.

[76] Opperman, L. A. (2000). Cranial sutures as intramembranous bone growth sites. *Developmental Dynamics: An Official Publication of the American Association of Anatomists*, *219*, 472–485.

[77] Jiang, X., Iseki, S., Maxson, R. E., Sucov, H. M., & Morriss-kay, G. M. (2002). Tissue Origins and Interactions in the Mammalian Skull Vault, *116*, 106–116.

[78] Chai, Y., Jiang, X., Ito, Y., Bringas, P., Han, J., Rowitch, D. H.,… Sucov, H. M. (2000). Fate of the mammalian cranial neural crest during tooth and mandibular morphogenesis. *Development (Cambridge, England)*, *127*, 1671–1679.

[79] Long, F. (2012). Building strong bones: molecular regulation of the osteoblast lineage. *Nature Publishing Group*, *13*(1), 27–38.

[80] Flaherty, K., Singh, N., & Richtsmeier, J. T. (2016). Understanding craniosynostosis as a growth disorder, *5*(August).

[81] Twigg, S. R. F., & Wilkie, A. O. M. (2015). (REVIEW) A Genetic-Pathophysiological Framework for Craniosynostosis. *The American Journal of Human Genetics*, *97*(3), 359–377.

[82] Bildsoe, H., Loebel, D. A. F., Jones, V. J., Hor, A. C. C., Braithwaite, A. W., Chen, Y., … Tam, P. P. L. (2013). The mesenchymal architecture of the cranial mesoderm of mouse embryos is disrupted by the loss of Twist1 function. *Developmental Biology*, *374*(2), 295–307.

[83] Kim, H.-J. (2003). Erk pathway and activator protein 1 play crucial roles in FGF2-stimulated premature cranial suture closure. *Dev. Dyn.;* **227**, 335–346.

[84] Tang, Yi et al. "Snail/Slug-YAP/TAZ Complexes Control Skeletal Stem Cell Self-Renewal and Differentiation." *Nature cell biology* 18.9 (2016): 917–929.